

# Efficient Sampling and Structure Learning of Bayesian Networks\*

**Jack Kuipers**

JACK.KUIPERS@BSSE.ETHZ.CH

**Polina Suter**

*D-BSSE, ETH Zurich, Mattenstrasse 26, 4058 Basel, Switzerland*

**Giusi Moffa**

*Division of Psychiatry, University College London, London, UK*

*Department of Mathematics and Computer Science, University of Basel, Basel, Switzerland*

## Abstract

Bayesian networks are probabilistic graphical models widely employed to understand dependencies in high dimensional data, and even to facilitate causal discovery. Learning the underlying network structure, which is encoded as a directed acyclic graph (DAG) is highly challenging mainly due to the vast number of possible networks. Efforts have focussed on two fronts: constraint-based methods that perform conditional independence tests to exclude edges and score and search approaches which explore the DAG space with greedy or MCMC schemes. Here we synthesise these two fields in a novel hybrid method which reduces the complexity of MCMC approaches to that of a constraint-based method. Individual steps in the MCMC scheme only require simple table lookups so that very long chains can be efficiently obtained. Furthermore, the scheme includes an iterative procedure to correct for errors from the conditional independence tests. The algorithm offers markedly superior performance to alternatives, particularly because DAGs can also be sampled from the posterior distribution, enabling full Bayesian model averaging for much larger Bayesian networks.

**Keywords:** Bayesian Networks, Structure Learning, MCMC.

## 1. Introduction

Bayesian networks are statistical models to describe and visualise in a compact graphical form the probabilistic relationships between variables of interest. The nodes of a graphical structure correspond to the variables, while directed edges between the nodes encode conditional independence relationships between them. The most important property of the digraphs underlying a Bayesian network is that they are acyclic, i.e. there are no directed paths which revisit any node. Such graphical objects are commonly denoted DAGs (directed acyclic graphs).

Alongside their more canonical use for representing multivariate probability distributions, DAGs also play a prominent role in describing causal models (Greenland et al., 1999; Pearl, 2000; Hernán and Robins, 2006; VanderWeele and Robins, 2007) and facilitating causal discovery from observational data (Maathuis et al., 2009; Moffa et al., 2017), though caution is warranted in their use and interpretation (Dawid, 2010). However, the potential for causal discovery and uncovering the mechanisms underlying scientific phenomena in dis-

---

\*. R package **BiDAG** is available at <https://CRAN.R-project.org/package=BiDAG>

ciplines ranging from the social sciences (Elwert, 2013) to biology (Friedman et al., 2000; Friedman, 2004; Kuipers et al., 2018) has driven interest in DAG inference.

To fully characterise a Bayesian network we need the DAG structure and the parameters which define an associated statistical model to explicitly describe the probabilistic relationships between the variables. To make any inference about the variables in the network, we need both components, the structure and the parameters, which we may need to estimate from data. Given sample data from the joint probability distribution on the node variables, learning the graphical structure is in general the more challenging task. The difficulty mostly rests with the mere size of the search space, which grows super-exponentially with the number of nodes  $n$ , since the logarithm grows quadratically (Robinson, 1970, 1973). A curious illustration of this growth is that the number of DAGs with 21 nodes is approximately the estimated number of atoms in the observable universe ( $\approx 10^{80}$ ).

### 1.1 Bayesian network notation

Bayesian networks represent a factorisation of multivariate probability distributions of  $n$  random variables  $\mathbf{X} = \{X_1, \dots, X_n\}$  by encoding conditional dependencies in a graphical structure. A Bayesian network  $\mathcal{B} = (\mathcal{G}, \theta)$  consists of a DAG  $\mathcal{G}$  and an associated set of parameters  $\theta$  which define the conditional distribution  $P(X_i \mid \mathbf{Pa}_i)$  of each variable  $X_i$  on its parents  $\mathbf{Pa}_i$ . The distribution represented by the Bayesian networks is then assumed to satisfy the *Markov property* (described for example in Koller and Friedman, 2009) that each variable  $X_i$  is independent of its non-descendants given its parents  $\mathbf{Pa}_i$ , allowing the joint probability distribution to factorise as

$$P(X_1, \dots, X_n) = \prod_i^n P(X_i \mid \mathbf{Pa}_i) \quad (1)$$

Learning the parameters  $\theta$  which best describe a set of data  $D$  for a given graph  $\mathcal{G}$  is generally straightforward for complete data, with the main difficulty in learning the structural dependence in  $\mathbf{X}$  and the DAG  $\mathcal{G}$  itself.

Due to the symmetry of conditional independence relationships, the same distribution might factorise according to different DAGs. DAGs encoding the same probability distribution constitute an equivalence class: they share the v-structures (two unconnected parents of any node, Verma and Pearl, 1990) and the skeleton (the edges if directions were removed). The equivalence class of DAGs can be represented as an essential graph (Andersson et al., 1997) or a completed partially directed acyclic graph (CPDAG) (Chickering, 2002b). Based purely on probabilistic properties, Bayesian networks can therefore only be learned from data up to an equivalence class.

### 1.2 DAG posteriors

In inferring Bayesian networks, the dual challenge consists of learning the graph structure (or its equivalence class) which best fits and explains the data  $D$ , and accounting for the uncertainty in the structure and parameters given the data. A natural strategy in Bayesian inference consists of sampling and averaging over a set of similarly well fitting networks. Each DAG  $\mathcal{G}$  is assigned a score equal to its posterior probability given the data  $D$

$$P(\mathcal{G} \mid D) \propto P(D \mid \mathcal{G})P(\mathcal{G})$$

where the likelihood  $P(D \mid \mathcal{G})$  has been marginalised over the parameter space. When the graph and parameter priors satisfy certain conditions of structure modularity, parameter independence and parameter modularity (Heckerman and Geiger, 1995; Friedman et al., 2000; Friedman and Koller, 2003) then the score decomposes as

$$P(\mathcal{G} \mid D) \propto P(D \mid \mathcal{G})P(\mathcal{G}) = \prod_{i=1}^n S(X_i, \mathbf{Pa}_i \mid D), \quad (2)$$

involving a function  $S$  which depends only on a node and its parents. For discrete categorical data, a Dirichlet prior is the only choice satisfying the required conditions for decomposition, leading to the BDe score of Heckerman and Geiger (1995). For continuous multivariate Gaussian data, the inverse Wishart prior leads to the BGe score (Geiger and Heckerman, 2002; corrected in Consonni and Rocca, 2012; Kuipers et al., 2014). In this manuscript we focus on the continuous case with the BGe score when evaluating the complexity of our approach, and discuss the discrete categorical case in Appendix C.

### 1.3 State of the art structure learning

Traditional approaches to structure learning fall into two categories (and their combination):

- constraint-based methods, relying on conditional independence tests
- score and search algorithms, relying on a scoring function and a search procedure

Below we provide a brief review of these concepts and algorithms of each class pertinent to this work.

#### 1.3.1 CONSTRAINT-BASED METHODS

Constraint-based methods exploit the property of Bayesian networks that edges encode conditional dependencies. If a pair of variables can be shown to be independent of each other when conditioning on at least one set (including the empty set) of the remaining variables, then a direct edge between the corresponding nodes in the graph can be excluded. The most prominent example of constraint-based methods is the well known PC algorithm of Spirtes et al. (2000), more recently popularised by Kalisch and Bühlmann (2007), who provided consistency results for the case of sparse DAGs and an **R** (R Core Team, 2017) implementation within the **pcalg** package (Kalisch et al., 2012).

Rather than exhaustively search the  $2^{(n-2)}$  possible conditioning sets for each pair of nodes, the crucial insight of the PC algorithm is to perform the tests in order of increasing complexity. Namely, starting from a fully connected (undirected) graph, the procedure tests marginal independence (conditioning on the empty set) for all pairs of nodes. Then it performs pairwise conditional independence tests between pairs of node which are still directly connected, conditioning on each adjacent node of either node in the pair, and so on conditioning on larger sets. Edges are always deleted when a conditional independence test cannot be rejected. This strategy differs from the typical use of hypothesis testing since edges are assumed to be present by default, but the null hypothesis is taken as conditional independence.

Edges which are never deleted through the process form the final skeleton of the PC algorithm. The conditional independencies which are not rejected identify all v-structures of the graph, fixing the direction of the corresponding edges. At this point it may still be possible to orient some edges, to ensure that no cycles are introduced and no additional v-structures are created (Meek, 1995). The algorithm finally returns the CPDAG of the Markov equivalence class consistent with the conditional dependencies compatible with the data.

In the final skeleton, for each node the remainder of its adjacent neighbourhood will have been conditioned upon. For the node with largest degree  $K$ , at least  $K2^{K-1}$  tests will have been performed and the algorithm is of exponential complexity in the largest degree. In the best case the algorithm may still run with  $K$  around 25–30, but in the worst case the base can increase giving a complexity bound of  $O(n^K)$  making the algorithm infeasible even for low  $K$  for large DAGs (Kalisch and Bühlmann, 2007).

For sparse large graphs, the PC algorithm can be very efficient. Despite the efficiency, since edges can only be deleted and many (correlated) independence tests are performed, the PC algorithm tends to have a high rate of false negatives and hence lose edges, so that it finds only a fraction of those in the true network (Uhler et al., 2013). Increasing the threshold for the conditional independence tests does little to alleviate the problem of false negatives while increasing runtime substantially. Another aspect of the problem of repeated tests is that the output of the PC algorithm can depend on the order of the tests (or the ordering of the input data), leading to unstable estimates in high dimensions, although modifications have been proposed to mollify this effect (Colombo and Maathuis, 2014).

### 1.3.2 SCORE AND SEARCH METHODS

On the other side of the coin are score and search methods and MCMC samplers. Each DAG gets a score, typically a penalised likelihood or a posterior probability (Section 1.2). An algorithm then searches through the DAG space for the structure (or ensemble thereof) which optimises the score, or to return a sample proportional to the score.

The most basic sampler is structure MCMC where each step involves adding, deleting or reversing an edge (Madigan and York, 1995; Giudici and Castelo, 2003) and accepting the move according to a Metropolis-Hastings probability. The scheme is highly flexible – amplifying the score leads to simulated annealing while modulating the amplification through the acceptance rate leads to adaptive tempering, to speed up the traversal and exploration of the DAG space. Sampling from the neighbourhood of DAGs with one edge added, removed or reversed, proportional to their scores results in faster MCMC convergence (as for example in Jennings and Corcoran, 2018). Greedy hill climbing instead proceeds by choosing the highest scoring DAG in the neighbourhood as the new starting point. Greedy equivalence search (GES) (Chickering, 2002a) is a popular algorithm for a greedy search approach on the space of Markov equivalent DAGs.

When the score is decomposable (as in Eq. (2)), only nodes whose parents change need to be rescored providing an  $O(n)$  speedup for structure based methods. Since the decomposability in Eq. (2) mimics the factorisation in Eq. (1) it is a property possessed by commonly used scores like the BIC penalised likelihood or the BDe or BGe, and an essential property for more advanced algorithms.

A direction spearheaded by order MCMC (Friedman and Koller, 2003) reduces the search space by combining large collections of DAGs together, namely all DAGs sharing the same topological ordering of the nodes. The score of the order consists of the sum of the scores of the DAGs consistent with it, and an MCMC scheme runs on the space of orders which are simply permutations of the  $n$  nodes. Although the number of DAGs compatible with each order also grows super-exponentially, the sum of all their scores involves  $\approx 2^n$  different contributions and can be evaluated in exponential time (Buntine, 1991). For larger  $n$  computations become quickly prohibitive and the complexity is artificially reduced to polynomial  $O(n^{K+1})$  by imposing a hard limit  $K$  on the number of parents allowed for each node. Nevertheless the strategy of combining large sets of DAGs and working on the much smaller (though still factorial) space of orders, enormously improves convergence with respect to structure MCMC, allowing the search and sampling of much larger graphs (for moderate or low  $K$ ).

Score decomposability is also necessary for order-based greedy search (Teyssier and Koller, 2005) as well as for dynamic or integer linear programming methods (Koivisto and Sood, 2004; Eaton and Murphy, 2007; He et al., 2016; Cussens, 2011; Cussens et al., 2017) for structure learning. For Bayesian model averaging, one limitation with order MCMC derives from the fact that DAGs may belong to multiple orders, introducing a bias in the sampling. The bias can be avoided by working on the space of ordered partitions (Kuipers and Moffa, 2017) which provide a unique representation of each DAG. Other MCMC alternatives include large scale edge reversal (Grzegorzczak and Husmeier, 2008) and Gibbs sampling (Goudie and Mukherjee, 2016) moves. Unbiased MCMC schemes, such as these, are currently the only viable approaches to sampling and accounting for structure uncertainty, though still limited to smaller or relatively sparse graphs.

As the size and connectivity of the target DAGs increase, the wide spectrum of constraint-based and score and search algorithms, cannot but fail to converge or discover optimally scoring graphs. To limit the extent to which the search space grows with the number of nodes, Friedman et al. (1999) pruned it by only allowing edges from selected candidate parents and performing a greedy search in the restricted search space. They also iteratively updated the set of candidate parents based on the current best DAG discovered. With the same aim of limiting the search space, Tsamardinos et al. (2006) brought together the ease of conditional independence testing and the performance of DAG searching, to benefit from their individual advantages. First a constraint-based method, akin to the PC algorithm, identifies a (liberal) undirected skeleton. A greedy search then acts on the restricted search space defined by excluding edges which are not included in the reference skeleton. Since score and search, when feasible, tends to perform better (Heckerman et al., 2006) than constraint-based methods, the hybrid approach of Tsamardinos et al. (2006) outperformed previous methods. Nandy et al. (2018) recently investigated the consistency properties of hybrid approaches using GES in high dimensional settings.

#### 1.4 Original contribution

In this work, we bring the power and sophistication of order and partition MCMC to the hybrid framework for structure learning. The result is a highly efficient algorithm for search and sampling with marked improvements on current state of the art methods. The key is to

observe that the exponential complexity in  $K$  of  $n^K$  for order or partition MCMC (Friedman and Koller, 2003; Kuipers and Moffa, 2017) derives from allowing among the potentially  $K$  parents of each node any of the other  $(n-1)$ . If the set of  $K$  potential parents is pre-selected, for example through a constraint-based method relying on conditional independence tests, the complexity reduces to  $2^K$  for searching of an optimal structure, and  $3^K$  for unbiased structure sampling. The complexity of the search then matches that of the testing component of the PC algorithm. Along with the standard pre-computation of parents set scores, which are exponentially costly, we introduce a method to also precompute tables of partial sums of parent set score with no complexity overhead. In particular we tabulate every score quantity needed for the MCMC scheme. During each MCMC step we then simply need to look up the relevant scores providing a very efficient sampler.

A distinctive feature of our method is not to fully trust the search space provided by the initial constraint-based method. Each node is entitled to have as parent any of the permissible nodes in the search space, and an additional arbitrary one from outside that set. Accounting for the expansion to the potential parent set, each MCMC step takes an expected time of order  $O(K)$ , despite scoring vast sets of DAGs at a time, and therefore comparable or even lower complexity than structure MCMC moves (between  $O(n)$  and  $O(n^2)$ , though some rejected moves can be  $O(1)$ ; Giudici and Castelo, 2003). The expansion beyond the skeleton provides a mechanism to iteratively improve the search space until it includes the maximally scoring DAG encountered, or the bulk of the posterior weight. Based on our simulations the results strongly outperform currently available alternatives, enabling efficient inference and sampling of much larger DAGs.

In Section 2 we develop efficient algorithms for order-based sampling for a known search space and examine their convergence. Then in Section 3 we demonstrate how to improve the search space iteratively, and show how this offers notably improved performance in finding the best DAG. Finally, we extend the scheme to the space of partitions to provide an unbiased sampler in Section 4, with discussions in Section 5. The algorithms introduced here are all implemented in the **R** (R Core Team, 2017) package **BiDAG**.

## 2. Order-based DAG sampling on a given search space

In the order MCMC algorithm of Friedman and Koller (2003), the  $n$  nodes of a DAG are arranged in topological order  $\prec$ . We associate a permutation  $\pi_{\prec}$  with each order. For a DAG to be compatible with an order, the parents of each node must have a higher index in the permutation

$$\mathcal{G} \in \prec \stackrel{\text{def}}{\iff} \forall i, \forall \{j : X_j \in \mathbf{Pa}_i\}, \pi_{\prec}[i] < \pi_{\prec}[j] \quad (3)$$

Visually, when we place the nodes in a linear chain from left to right according to  $\pi_{\prec}$ , edges may only come from nodes further to the right (Figure 1b). With the rows and columns labelled following  $\pi_{\prec}$ , the adjacency matrix of a compatible DAG is lower triangular so that a total of  $2^{\binom{n}{2}}$  DAGs are compatible with each order.

### 2.1 Order MCMC

The idea of order MCMC is to combine all DAGs consistent with an order to reduce the problem to the much smaller space of permutations instead of working directly on the space

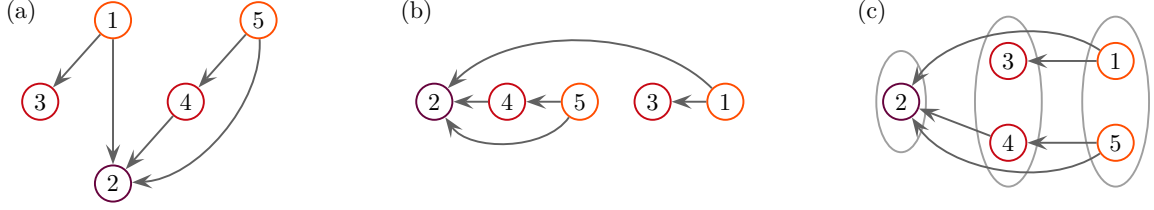


Figure 1: The DAG in (a) is compatible with the order depicted in (b), as edges only originate from nodes further right in the chain, along with 8 other orders. The DAG however can be uniquely assigned to a labelled partition by collecting outpoints into partition elements to arrive at the representation in (c).

of DAGs. Each order  $\prec$  receives a score  $R(\prec | D)$  equal to the sum of the scores of all DAGs in the order

$$R(\prec | D) = \sum_{\mathcal{G} \in \prec} P(\mathcal{G} | D) \quad (4)$$

Instead of naively scoring all DAGs in an order, Friedman and Koller (2003) used the factorisation in Eq. (2)

$$R(\prec | D) \propto \sum_{\mathcal{G} \in \prec} \prod_{i=1}^n S(X_i, \mathbf{Pa}_i | D) = \prod_{i=1}^n \sum_{\mathbf{Pa}_i \in \prec} S(X_i, \mathbf{Pa}_i | D) \quad (5)$$

to exchange the sum and product (following Buntine, 1991). The sum is restricted to parent subsets compatible with the node ordering

$$\mathbf{Pa}_i \in \prec \stackrel{\text{def}}{\iff} \forall \{j : X_j \in \mathbf{Pa}_i\}, \pi_{\prec}[i] < \pi_{\prec}[j] \quad (6)$$

The score of the order therefore reduces to sums over all compatible parent subsets, eliminating the need of summing over DAGs. For a node with  $k$  possible parents further along the order, there are  $2^k$  parents subsets. Evaluating the score of the order therefore requires  $\sum_{k=0}^{n-1} 2^k = (2^n - 1)$  evaluations of the score function  $S$ . This provides a massive reduction in complexity compared to scoring all  $2^{\binom{n}{2}}$  DAGs in the order individually. The exponential complexity in  $n$  is still too high for larger DAGs so a hard limit  $K$  on the size of the parent sets is typically introduced to obtain polynomial complexity of  $O(n^{K+1})$  evaluations of  $S$ . For larger DAGs however,  $K$  must be rather small in practice, so that the truncation runs the risk of artificially excluding highly scoring DAGs. As a remedy, we start by defining order MCMC on a given search space, which may be selected for example based on prior subject knowledge or from a skeleton derived through constraint-based methods.

## 2.2 Restricting the search space

The search space can be defined by a directed graph  $\mathcal{H}$ , which is not necessarily acyclic, or its adjacency matrix,  $H$ :

$$H_{ji} = 1 \text{ if } \{j, i\} \in \mathcal{H} \quad (7)$$

One advantage with respect to simply using an undirected skeleton, which corresponds to a symmetric matrix, is that the directed graph naturally allows for prior information about edge directionality to be included. Prior beliefs about undirected edges can also be included by treating both directions equally. In the search space, each node has the following set of permissible parents

$$\mathbf{h}^i = \{X_j : H_{ji} = 1\} \quad (8)$$

For a set of size  $K$  we evaluate the score of each possible combination and store the scores in a table (as in the example on the left of Table S1) as is standard practice. Since there are  $2^K$  possible combinations, and for the BGe score each involves taking the determinant of a matrix, the complexity of building this table is  $O(K^3 2^K)$ . For convenience later, we label the different scores with a binary mapping from a parent subset  $\mathbf{Z}$  to the integers:

$$f(\mathbf{Z}) = \sum_{j=1}^K I(h_j^i \in \mathbf{Z}) 2^{j-1} \quad (9)$$

using the indicator function  $I$ .

### 2.3 Efficient order scoring

To score all the DAGs compatible with a particular order we still need to select and sum the rows in the score tables where the parent subset respects the order

$$R_{\mathcal{H}}(\prec | D) \propto \prod_{i=1}^n \sum_{\substack{\mathbf{Pa}_i \subseteq \mathbf{h}^i \\ \mathbf{Pa}_i \in \prec}} S(X_i, \mathbf{Pa}_i | D) \quad (10)$$

with the additional constraint that all elements in the parent sets considered must belong to the search space defined by  $\mathcal{H}$ . From the precomputed score table of all permissible parent subsets in the search space, we select those compatible with the order constraint. Simply running through the  $2^K$  rows takes exponential time (in  $K$ ) for each node. Unlike other order-based schemes, we can avoid this by building a second table: the summed score table (see the example on the right of Table S1).

In Appendix A we detail the algorithmic steps which allow us to build the summed score table for each variable with a complexity of  $O(K^2 2^K)$ . Compared to the complexity of building the original score table of  $O(K^3 2^K)$ , this step adds no complexity overhead to the method. The summed score table however provides the means to efficiently score each order. For each node we look up the relevant row in the summed score table and by moving linearly along the order we can compute Eq. (10) in  $O(Kn)$  as

$$R_{\mathcal{H}}(\prec | D) \propto \prod_{i=1}^n \Sigma_{f(\mathbf{h}^i \in \prec)}^i \quad (11)$$

where

$$\mathbf{h}^i \in \prec \stackrel{\text{def}}{=} \{X_j \in \mathbf{h}^i : \pi_{\prec}[i] < \pi_{\prec}[j]\} \quad (12)$$



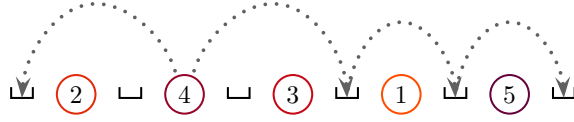


Figure 2: For any randomly chosen node, here 4, we score the entire neighbourhood of new positions in the order by performing a sequence of local transpositions and include the known score of the current position. The new placement is sampled proportionally to the scores of the different orders in the neighbourhood.

are the elements of  $\mathbf{h}^i$  compatible with the order constraints and

$$\Sigma_{f(\mathbf{h}^i \in \prec)}^i = \sum_{\substack{\mathbf{Pa}_i \subseteq \mathbf{h}^i \\ \mathbf{Pa}_i \in \prec}} S(X_i, \mathbf{Pa}_i \mid D) \quad (13)$$

is the sum of scores of all the parent sets in the search space respecting the order, which is precomputed using Algorithm S1.

## 2.4 Order MCMC moves

The strategy of order MCMC is to build a Markov chain on the space of orders. From the order  $\prec_t$  at the current iteration  $t$ , a new order  $\prec'$  is proposed and accepted with probability

$$\rho = \min \left\{ 1, \frac{R_{\mathcal{H}}(\prec' \mid D)}{R_{\mathcal{H}}(\prec_t \mid D)} \right\} \quad (14)$$

to provide a chain with a stationary distribution proportional to the score  $R_{\mathcal{H}}(\prec \mid D)$  for symmetric proposals. The standard proposal (Friedman and Koller, 2003) is to swap two nodes in the order while leaving the others fixed. We will denote this move as a *global swap*. The set of permissible parents of all nodes between the two swapped ones may change, requiring them to be rescored. Computing the score of the proposed order then has a complexity  $O(n)$ . It is possible to move from one order to any other in  $(n - 1)$  steps (assuming non-zero order scores), making the chain irreducible. A more local move of only transposing two adjacent nodes allows the proposed order to be scored in  $O(1)$ . We will denote this move as a *local transposition* which takes  $O(n^2)$  steps to have access to any order.

### 2.4.1 A GIBBS MOVE IN ORDER SPACE

On the space of orders we define a new move with the same complexity of the standard global swap move and denote it as a *node relocation*. From the current state in the chain,  $\prec_t$ , first sample a node uniformly from the  $n$  available, say node  $i$ . For the move we sample the position of node  $i$  conditional on keeping the relative ordering of the remaining nodes unchanged. Define the neighbourhood of the order under this move,  $\text{nb}d^i(\prec_t)$ , to be all orders with node  $i$  placed elsewhere in the order or at its current position, as in the example in Figure 2 with node 4 chosen. To move through the full neighbourhood of size

---

**Algorithm 1** Node relocation move in the space of orders
 

---

**input** The order  $\prec_t$  at step  $t$  of the chain  
 Sample node  $i$  uniformly from the  $n$   
 Build and score all orders in the neighbourhood  $\text{nb}d^i(\prec_t)$ ,  
     through consecutive local transpositions of node  $i$   
 Sample proposed order  $\prec'$  from  $\text{nb}d^i(\prec_t)$  proportionally to  $R_{\mathcal{H}}(\prec' | D)$   
 Set  $\prec_{t+1} = \prec'$   
**return**  $\prec_{t+1}$

---

$n$ , we can sequentially transpose node  $i$  with adjacent nodes. Since each local transposition takes a time  $O(1)$  to compute the score of the next order, scoring the whole neighbourhood takes  $O(n)$ . Finally sample a proposed order  $\prec'$  proportionally to the scores of all the orders in the neighbourhood. As a consequence the move is always accepted and the next step of the chain set to the proposed order  $\prec_{t+1} = \prec'$ . We summarise the move in Algorithm 1.

The newly defined node relocation move satisfies detailed balance

$$P(\prec' | \prec) R_{\mathcal{H}}(\prec | D) = P(\prec | \prec') R_{\mathcal{H}}(\prec' | D) \quad (15)$$

where  $P(\prec' | \prec)$  is the transition probability from  $\prec$  to  $\prec'$ . The transition involves first sampling a node  $i$  and then the order proportionally to its score so that (for orders not connected by a local transposition)

$$P(\prec' | \prec) = \frac{1}{n} \frac{R_{\mathcal{H}}(\prec' | D)}{\sum_{\prec'' \in \text{nb}d^i(\prec)} R_{\mathcal{H}}(\prec'' | D)} \quad (16)$$

The reverse move needs the same node  $i$  to be selected, and as  $\text{nb}d^i(\prec) = \text{nb}d^i(\prec')$  the denominators cancel when substituting into Eq. (15). For orders connected by a local transposition, say node  $i$  swapped with the adjacent node  $j$ , there are two possible paths connecting the orders and a transition probability of

$$P(\prec' | \prec) = \frac{1}{n} \frac{R_{\mathcal{H}}(\prec' | D)}{\sum_{\prec'' \in \text{nb}d^i(\prec)} R_{\mathcal{H}}(\prec'' | D)} + \frac{1}{n} \frac{R_{\mathcal{H}}(\prec' | D)}{\sum_{\prec'' \in \text{nb}d^j(\prec)} R_{\mathcal{H}}(\prec'' | D)} \quad (17)$$

Since the reverse move involves the same pair of nodes, we can again directly verify detailed balance by substituting into Eq. (15).

The move is aperiodic since the original order is included in the neighbourhood. It is possible to reach any order from any other by performing  $(n - 1)$  steps making the chain also irreducible. Therefore the newly defined move satisfies the requirements for the chain to converge and provide order samples from a probability distribution proportional to the score  $R_{\mathcal{H}}(\prec | D)$ .

The node relocation move naturally provides a fixed scan Gibbs sampler by cycling through the nodes sequentially, rather than sampling at each step.

#### 2.4.2 CHAIN COMPLEXITY

We mix the three moves into a single scheme. Since the global swap involves rescoreing  $\approx \frac{n}{3}$  nodes on average at each step, while the local transposition involves 2 and the node

relocation  $2n$  we can keep the average complexity at  $O(1)$  if we sample the more expensive moves with a probability  $\propto \frac{1}{n}$ . In this way, we can also balance their computational costs. For simplicity we assign each move equal average computational time by selecting them with a probability of  $(\frac{6}{n}, \frac{n-7}{n}, \frac{1}{n})$  respectively. With the mixture of moves, the number of steps to reach any order is  $O(n)$  so following the heuristic reasoning of Kuipers and Moffa (2017) we would expect convergence of the chain to take  $O(n^2 \log(n))$  steps. This complexity is consistent with our simulation results (Figure 3).

Once the score tables have been computed, the complexity of running the whole chain is also  $O(n^2 \log(n))$ . Utilising the lookup table of summed scores therefore reduces the complexity substantially by a factor of  $O(n^K)$  compared to standard order MCMC where one simply restricts the size of parent sets to  $K$  and only utilises the basic score tables.

### 2.4.3 DAG SAMPLING

To draw a DAG consistent with a given sampled order, we can sample the parents of each node proportionally to the entries respecting the order in the score table. Complexity remains exponential, of  $O(2^K)$ , so the scheme should be thinned such that DAG sampling only happens periodically in the order chain. The frequency should be set so that sampling takes computational time at most comparable to running the order chain inbetween.

## 2.5 Extending the search space

The restricted search space, derived for example through constraint-based methods, may exclude relevant edges. To address this problem, we extend our approach by softening the restrictions. In particular we allow each node to have one additional parent from among the nodes outside its permissible parent set. The score of each order becomes

$$R_{\mathcal{H}}^+(\prec | D) \propto \prod_{i=1}^n \sum_{\substack{\mathbf{Pa}_i \subseteq \mathbf{h}^i \\ \mathbf{Pa}_i \in \prec}} \left[ S(X_i, \mathbf{Pa}_i | D) + \sum_{\substack{X_j \notin \mathbf{h}^i \\ \pi_{\prec}[i] < \pi_{\prec}[j]}} S(X_i, \{\mathbf{Pa}_i, X_j\} | D) \right] \quad (18)$$

For the efficient computation of the sum, we build a score table for each node and each additional parent. For a node with  $K$  parents this leads to  $(n - K + 1)$  tables in total and we perform Algorithm S1 of Appendix A on each of them. The time and space complexity of building these tables is therefore an order  $n$  more expensive than using the restricted search space. Given the tables, however, an order can again be scored with a simple lookup

$$R_{\mathcal{H}}^+(\prec | D) \propto \prod_{i=1}^n \left[ \Sigma_{f(\mathbf{h}^i \in \prec)}^i + \sum_{\substack{X_j \notin \mathbf{h}^i \\ \pi_{\prec}[i] < \pi_{\prec}[j]}} \Sigma_{f(\mathbf{h}^i \in \prec)}^{ij} \right] \quad (19)$$

where we also index the summed scores with the additional parent

$$\Sigma_{f(\mathbf{h}^i \in \prec)}^{ij} = \sum_{\substack{\mathbf{Pa}_i \subseteq \mathbf{h}^i \\ \mathbf{Pa}_i \in \prec}} S(X_i, \{\mathbf{Pa}_i, X_j\} | D), \quad X_j \notin \mathbf{h}^i \quad (20)$$

The complexity of scoring the order is  $O(n^2)$ .

### 2.5.1 MOVE COMPLEXITY

For the local transposition where we swap two adjacent nodes in the order, if neither is in the permissible parent set of the other we simply update one element of the sum in Eq. (19) in  $O(1)$ . If either is in the permissible parent set, all terms need to be replaced in  $O(n)$ . However since the nodes have up to  $K$  parents, the probability of a permissible parent being affected is  $\propto \frac{K}{n}$  giving an average complexity of  $O(K)$ . For the global swap the maximum complexity is  $O(n^2)$  when many of the intermediate nodes have among their permissible parents either of the swapped nodes, but on average the complexity is  $O(Kn)$  following the same argument as above. The node relocation move has the same complexity, so that the weighted mixture of moves typically takes just  $O(K)$ .

## 2.6 Convergence

To examine the convergence of our MCMC scheme, we ran simulations as described in Appendix B, and for each simulation repetition we compared two independent runs with different random initial points in the final search space for each dataset. We computed the squared correlation  $\rho^2$  of the two runs between the posterior probabilities of each edge, after excluding a burn-in period of 20%. Since most edges are absent, only edges with a posterior probability greater than 5% in at least one run were included. The median  $\rho^2$  along with the first and third quartiles are displayed in Figure 3. By scaling the number of MCMC steps with  $n^2 \log(n)$  we observe the correlation approaching 1. To examine the behaviour in more detail, we can consider  $(1 - \rho^2)^{-1}$  which increases roughly linearly with the scaled number of steps. We see, especially, that there is little dependence on the size of the network, apart from a slower convergence for the smallest network size. With reasonable consistency, and importantly no obvious decrease in scaled performance as the number of variables  $n$  increases, the simulation results of Figure 3 are in line with the estimate of requiring  $O(n^2 \log(n))$  steps for the MCMC convergence. Similar insensitivity to the network size is also visible for the root mean square error between runs (Figure S3).

## 3. Search space and maximal DAG discovery

In order to sample DAGs effectively, our search space needs to cover the bulk of the posterior weight. We describe here an iterative scheme to search for the highest scoring DAG in the current extended search space, and use it to update and improve the search space itself.

### 3.1 Maximal DAG discovery

In addition to sampling DAGs, we can also employ the MCMC scheme to search for the maximally scoring or maximum a posteriori (MAP) DAG. To this end (and analogously to Teyssier and Koller, 2005) we replace the score of each order by the score of the highest scoring DAG in that order

$$Q_{\mathcal{H}}(\prec | D) = \max_{\substack{\mathcal{G} \subseteq \mathcal{H} \\ \mathcal{G} \in \prec}} P(\mathcal{G} | D) \propto \prod_{i=1}^n \max_{\substack{\mathbf{Pa}_i \subseteq \mathbf{h}^i \\ \mathbf{Pa}_i \in \prec}} S(X_i, \mathbf{Pa}_i | D) \quad (21)$$

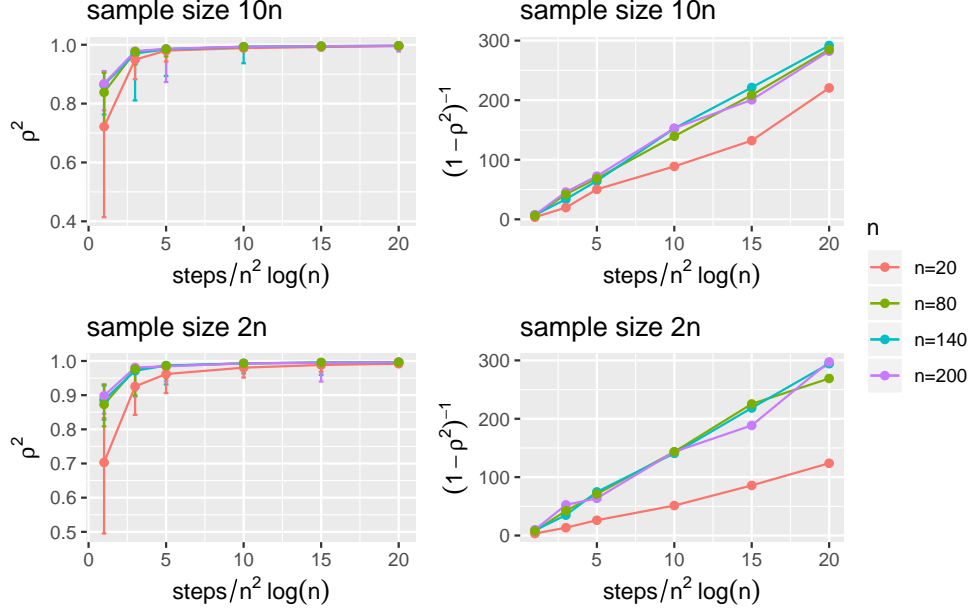


Figure 3: The correlation between edge probabilities from different runs as the size of the network increases. The simulation setting is described in Appendix B. The number of steps in the chain is scaled by  $n^2 \log(n)$ . The transformation on the right highlights the roughly linear improvement in the convergence measure with the number of steps and that there is little dependence on the network size.

To compute the terms on the right we again follow the steps detailed in Appendix A using the Hasse power set representation of the permissible parent set of each node and propagating the maximum of scores down the power set following Algorithm S2 of Appendix A:

$$Q_{\mathcal{H}}(\prec | D) \propto \prod_{i=1}^n M_{f(\mathbf{h}^i \in \prec)}^i, \quad M_{f(\mathbf{h}^i \in \prec)}^i = \max_{\substack{\mathbf{Pa}_i \subseteq \mathbf{h}^i \\ \mathbf{Pa}_i \in \prec}} S(X_i, \mathbf{Pa}_i | D) \quad (22)$$

### 3.1.1 STOCHASTIC SEARCH

Finding the order with the highest  $Q$  directly provides a MAP DAG. A stochastic search based on the order MCMC scheme with score  $Q_{\mathcal{H}}(\prec | D)$  can tackle the problem. Running the scheme, we keep track of the highest scoring order, and hence the highest scoring DAG, encountered. The convergence time to sample orders from a distribution proportional to  $Q_{\mathcal{H}}(\prec | D)$  is again expected to be  $O(n^2 \log(n))$ .

To perform adaptive tempering and speed up discovery of a MAP DAG, we can transform the score by raising it to the power of  $\gamma$  and employ  $Q_{\mathcal{H}}(\prec | D)^\gamma$ . This transformation smooths ( $\gamma < 1$ ) or amplifies ( $\gamma > 1$ ) the score landscape and the value of  $\gamma$  can be tuned adaptively depending on the acceptance probability of the MCMC moves while running the

algorithm. To effectively explore local neighbourhoods, the target acceptance of swaps may scale  $\propto \frac{1}{n}$ . Alternatively, simulated annealing can be performed by sending  $\gamma \rightarrow \infty$ .

### 3.1.2 GREEDY SEARCH

The order-based scheme can also be adapted to perform a greedy search (Teyssier and Koller, 2005). For example we score all possible  $(n - 1)$  local transpositions of adjacent nodes in  $O(n)$  and select the highest scoring at each step. Since it takes  $O(n^2)$  steps to be able to reach any order with this move, we would expect  $O(n^3)$  complexity to find each local maximum. For the global swap of two random nodes, scoring the neighbourhood itself is  $O(n^3)$  so that the  $O(n)$  to traverse the space makes this move more expensive than local transpositions. Local transpositions would therefore be generally preferable for greedy search, although global swaps may be useful to escape from local maxima.

The new node relocation move of moving a single node at a time (Figure 2) requires only  $O(n^2)$  to score all the possible new placements of all nodes. With  $O(n)$  steps to move between any pair of DAGs, we are again looking at  $O(n^3)$  complexity for each search. The new move also contains all local transpositions in its neighbourhood and so provides a complementary alternative to a greedy search scheme purely based on local transpositions.

## 3.2 Iteratively improving the search space

Extending the search space, so that each node may have an additional parent outside, allows us to discover edges which improve the score of DAGs, or edges with a high posterior weight (those which occur in a large fraction of sampled DAGs), which were previously excluded from the core search space defined by  $\mathcal{H}$ . Incorporating these edges into the core search space, we can iteratively improve the search space. This is analogous to the iterative updating of Friedman et al. (1999), but adapted to the order-based setting.

Starting with the original core search space  $\mathcal{H}_0 = \mathcal{H}$  we expand to allow one additional parent and search for the maximally scoring DAG in that space and convert it to the CPDAG  $\mathcal{G}_0^*$ . For the next core search space  $\mathcal{H}_1$  we take the union of the edges in  $\mathcal{H}$  and  $\mathcal{G}_0^*$ , expand and search for the highest scoring CPDAG  $\mathcal{G}_1^*$  in the new space. We iteratively repeat this procedure

$$\mathcal{H}_{i+1} = \mathcal{H} \cup \mathcal{G}_i^* \tag{23}$$

until no higher scoring CPDAG is uncovered and the last  $\mathcal{G}_i^*$  is entirely included in the core search space ( $\mathcal{H}_i = \mathcal{H} \cup \mathcal{G}_i^*$ ).

## 3.3 Performance

To illustrate the performance of our structure learning and sampling, we performed detailed simulations in Appendix B, and highlight here in Figure 4 the improvement that iteratively updating the search space and then sampling from it has over alternatives which apply to the size and density of networks we consider.

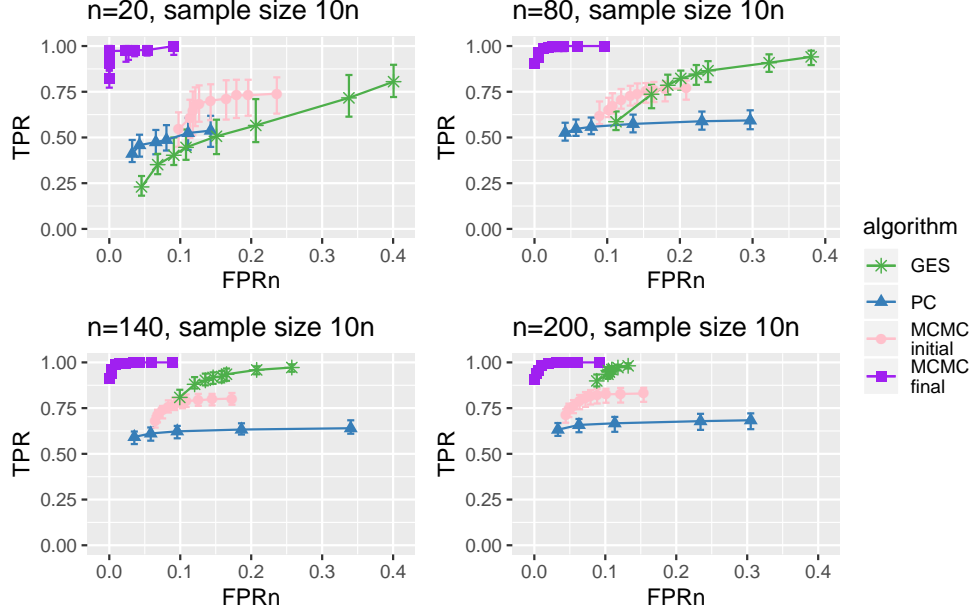


Figure 4: The performance in recovering the underlying DAG skeleton of our MCMC scheme (purple squares for different posterior thresholds) after converging to a core search space which contains the maximally scoring DAG encountered, compared to the PC algorithm (blue triangles for different significance levels) and GES (green stars for different likelihood penalisations). For completeness we include the results of our MCMC scheme when forced to use the expanded initial search skeleton from the PC algorithm (pink circles).

#### 4. Unbiased DAG sampling on a fixed search space

The order-based sampling scheme with a reduced search space (Section 2) can be modified to work with partition MCMC (Kuipers and Moffa, 2017) instead of order MCMC to obtain an unbiased sample of DAGs.

For partition MCMC, the nodes of a DAG are assigned to a labelled ordered partition  $\Lambda = (\lambda, \pi_\lambda)$  consisting of a partition  $\lambda$  of the  $n$  nodes and a permutation  $\pi_\lambda$  where the nodes within each partition element take ascending order. This provides a unique representation of each DAG unlike the simpler order representation which has a bias towards DAGs which belong to multiple orders. The assignment can be performed by recursively tracking nodes with no incoming edges, called outpoints (Robinson, 1970, 1973). In Figure 1 the outpoints are nodes 1 and 5 which are placed in the rightmost partition element. With these nodes and their outgoing edges removed, nodes 3 and 4 become outpoints placed into the second partition element and finally node 2 fills the remaining partition element. The partition is  $\lambda = [1, 2, 2]$  with permutation  $\pi_\lambda = 2, 3, 4, 1, 5$ .

When reversing the process and building a DAG recursively, the outpoints at each stage must be connected to from outpoints at the next stage. Each node in any partition element

must have at least one incoming edge from nodes in the adjacent partition element to the right, if there is one. For example, node 2 in any DAG compatible with the partition in Figure 1(c) must have an edge from either node 3 or node 4 (or both). Additional edges may only come from nodes further right.

There are then 12 possible incoming edge combinations for node 2, three for each of node 3 and 4, giving a total of 108 DAGs compatible with the labelled ordered partition of the DAG in Figure 1(c). In partition MCMC the sum of the scores of all these DAGs is assigned to the partition. We now describe an efficient implementation when the search space is restricted.

#### 4.1 Scoring partitions on a restricted search space

The posterior probability of a labelled partition is the sum of posterior probabilities of DAGs within the search space compatible with the partition

$$P_{\mathcal{H}}(\Lambda \mid D) = \sum_{\substack{\mathcal{G} \subseteq \mathcal{H} \\ \mathcal{G} \in \Lambda}} P(\mathcal{G} \mid D) \propto \prod_{i=1}^n \sum_{\substack{\mathbf{Pa}_i \subseteq \mathbf{h}^i \\ \mathbf{Pa}_i \in \Lambda}} S(X_i, \mathbf{Pa}_i \mid D) \quad (24)$$

where the restriction on parents sets induced by the partition is that they must contain at least one node from the adjacent partition element to the right. To evaluate the sums in Eq. (24) for each subset of banned nodes (belonging to the same partition element or further left) we need to keep track of the subset of *needed* nodes belonging to the partition element immediately to the right to ensure at least one is in the parent set. With  $K$  permissible parents for node  $i$  we have  $3^K$  possible subset pairs for which we use the ternary mapping:

$$g(\mathbf{Z}, \mathbf{W}) = \sum_{j=1}^K I(h_j^i \in \mathbf{Z}) 3^{j-1} + 2 \sum_{j=1}^K I(h_j^i \in \mathbf{W}) 3^{j-1} \quad (25)$$

with  $\mathbf{Z}$  representing the permissible parents, and  $\mathbf{W}$  those of which at least one must be present.

We detail the algorithmic steps to compute these sums efficiently in Appendix A and Algorithm S3 with a complexity of  $O(K^2 3^K)$ . The restriction encoded by partitions to remove the bias of order MCMC therefore increases the computational cost of building the lookup tables for the partition MCMC sampler. However, once the score table is built, computing the score of any partition from Eq. (24) reduces to

$$P_{\mathcal{H}}(\Lambda \mid D) \propto \prod_{i=1}^n \tilde{\Sigma}_{g(\mathbf{h}^i \in \Lambda, \mathbf{h}^i \in \lambda_i)}^i, \quad \tilde{\Sigma}_{g(\mathbf{h}^i \in \Lambda, \mathbf{h}^i \in \lambda_i)}^i = \sum_{\substack{\mathbf{Pa}_i \subseteq \mathbf{h}^i \\ \mathbf{Pa}_i \in \Lambda}} S(X_i, \mathbf{Pa}_i \mid D) \quad (26)$$

where  $\lambda_i$  represents the partition element containing node  $i$ . The score of the partition can be evaluated in  $O(Kn)$  from the lookup tables.



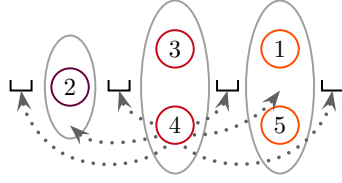


Figure 5: For any randomly chosen node, here 4, we score the entire neighbourhood of new positions by sequentially moving the node into different partition elements or the gaps inbetween. The new placement is sampled proportionally to the scores of the different labelled ordered partitions in the neighbourhood.

## 4.2 Partition MCMC moves

The simplest move in the partition space consists of splitting partition elements, or joining adjacent ones. Proposing such a move from  $\Lambda$  to  $\Lambda'$  and accepting with probability

$$\rho = \min \left\{ 1, \frac{\# \text{nb}(\Lambda) P_{\mathcal{H}}(\Lambda' | D)}{\# \text{nb}(\Lambda') P_{\mathcal{H}}(\Lambda | D)} \right\}, \quad (27)$$

while accounting for the neighbourhood sizes (following Kuipers and Moffa, 2017) is sufficient to sample partitions proportionally to their posterior probability in the search space. Nodes in two partition elements need to be rescored by looking up new values in their restricted sum tables. Although partition elements can get to a size  $O(n)$ , on average they contain around 1.5 nodes (Kuipers and Moffa, 2015) so we would expect  $O(1)$  for this move. Once a partition has been sampled, a compatible DAG can be sampled conditionally.

To speed up convergence, additional permutation moves were included in Kuipers and Moffa (2017), either between two nodes in adjacent partition elements, requiring again the rescoreing of nodes in two partition elements, or between any two nodes in different partition elements requiring the rescoreing of all nodes inbetween as well. We would typically expect  $O(1)$  for the local swapping of nodes and  $O(n)$  for the global swapping. The global swap is picked with a probability  $\propto \frac{1}{n}$  to contain the average complexity.

A final move is to select a single node and to move it elsewhere in the partition, or as a new partition element. Analogously to the single node move introduced in Section 2.4 we can score the entire neighbourhood for any node selected at random by sequentially moving it through the partition, as in Figure 5. Since each other node has its needed or banned parent sets essentially affected twice, scoring the neighbourhood takes  $O(n)$ . We always accept this move as it is sampled directly from the neighbourhood (which includes the starting partition), further aiding convergence. This move is also selected with a probability  $\propto \frac{1}{n}$ .

## 4.3 Expanding the search space

When expanding the search space, for each node we simply create further summed score tables where each time we include one other node from outside the search space as an additional parent. The space and time complexity increase by a factor of  $n$  when building

these tables. Since only one element is required from the needed node subsets defined by the adjacent partition element to the right, we sum over the relevant entries for all nodes outside the search space but in the adjacent partition element. For the MCMC moves, the time complexity can increase by a factor  $O(n)$  but the typical increase is again  $O(K)$  on average.

## 5. Discussion

In this work we presented a novel and computationally efficient approach for learning and sampling the DAGs underlying high dimensional Bayesian network models. Two main original features are worth highlighting:

First, the computational efficiency we gain by observing that every score quantity needed for the MCMC scheme can be effectively precomputed and stored in lookup tables. This goes beyond the common strategy in DAG inference of simply storing the scores of individual parent sets by additionally storing all sums of parent set scores, with no complexity overhead. This allows us to sink the complexity class of methods where we reduce the search space by grouping DAGs to score collectively, as in order-based approaches. Specifically, we reduce the main complexity bottleneck of  $n^K$  to just  $2^K$  or  $3^K$  which provides a massive computational advantage for larger and denser networks. Order and partition MCMC constitute the building blocks of our procedure with the further advantage that each step in the chain now takes minimal computational time.

Second, the improved accuracy in the inference of the network structure, achieved by means of an iterative expansion of the search space beyond the preliminary skeleton obtained through constraint-based methods. In fact the pre-defined search space may not include DAGs corresponding to the mode of the posterior distribution, so that hybrid methods can heavily benefit from the additional flexibility. The simulation studies (Appendix B) extensively demonstrate the improved performance we can achieve with respect to current mainstream approaches.

When iteratively updating the search space, we include edges ensuring that the highest scoring DAG found at each stage belongs to the core search space for the next iteration. Alternatively we could sample from the posterior distribution and update the search space by adding edges with a certain posterior probability. The order-based sample is of course biased, but the additional restriction in the combinatorics of partition MCMC, which ensures a unique representation of each DAG, increases the complexity of building the necessary lookup tables. For denser networks it may be preferable to pursue bias removal only at later iterations, once the search space has already converged under order. Finding the highest scoring DAG or sampling with order MCMC share the same complexity. We chose to update the search space based on the highest scoring DAG since order MCMC may find a maximal score faster than sampling, thanks to the possibility of tempering.

The freedom to add edges beyond a pre-defined skeleton, allows for the correction of errors where edges may be missed. The iterative approach is, aside from stochastic fluctuations in the search or sampling, mainly deterministic. However, since we only consider the addition of a single parent at a time for each node, the algorithm may not pick up missing correlated edges, which would only improve the score if added at the same time. Allowing for the concomitant addition of edge pairs increases the overall space complexity by a

factor  $n$  which can be computationally prohibitive. On the other hand we could view the search space itself, or the lists of permitted parents, as a random variable and implement a stochastic updating scheme. Especially for sparser graphs, such a scheme may be effective at extending the posterior sample outside of a fixed search space.

As the initial core search space we adopted the undirected skeleton obtained from the PC algorithm, without accounting for any orientations. The iterative steps of building the score tables have exponential complexity in the number of parents. In the case of nodes with many children, which will be included as potential parents, ignoring the direction will lead to increased costs in building the lookup tables. In certain cases it may therefore be convenient to limit permissible parent sets of particular nodes to those compatible with directed or undirected edges in the CPDAG learned through the PC algorithm.

Despite our focus on taking the skeleton given by the PC algorithm as the initial core search space, our approach is agnostic to the method used to define the starting point, although obviously performance will improve the closer the initial search space is to the target space containing the bulk of the posterior distribution. If relevant edges are missing in the initial search space, our algorithm can add them though it may take a few iterations to do so. False positive edges in the search space do not affect the MCMC search, but do increase the time and space needed for computing the lookup tables. In our simulations, the PC algorithm was quite conservative, even when relaxing the significance threshold, missing many edges but introducing few false positives. Due to the large number of missing edges, improving the search space tended to require quite a few iterations, which were however reasonably fast.

Defining the initial core search space by GES would include more of the important edges to start with, but also many false positives. As a consequence the algorithm would potentially require fewer steps to improve the search space, at the expense of higher computational cost of each step. In the context of GES, the number of false positives is sensitive to the penalisation parameter in the score, so ideally we should optimally tune it if using GES to define the initial search space. Order-based conditional independence tests also offer another option (Raskutti and Uhler, 2018). For Gaussian models, the Markov random field or conditional independence graph defined by the precision matrix (as used for example in Nandy et al., 2018) is also a possibility. Theoretically the conditional independence graph should contain all edges present in the PC algorithm skeleton, potentially including more true positive edges, while most likely also introducing additional false positives. In principle one may even combine search spaces from different approaches.

Interesting direction may also come from the ILP method of Cussens (2011) and Cussens et al. (2017), if the solver manages to complete and the number of parents in the maximally scoring DAG is less than the low limit needed for their input score tables. By expanding such a DAG appropriately, we may obtain a good starting point for the full sampling. Conversely, the final search space obtained by our search could be an interesting input for the ILP, or may be determined by combining elements of both approaches. Similarly one may investigate whether one can modify dynamic programming approaches for exhaustively searching orders (Koivisto and Sood, 2004; Silander and Myllymäki, 2006; Eaton and Murphy, 2007; He et al., 2016) to work on restricted search spaces and be efficient enough to replace the MCMC search.

Regardless of how we define the initial search space, or how we discover the maximal DAG, our hybrid scheme is the only one capable of efficiently sampling larger and denser graphs. Sampling from the posterior distribution not only improves structure learning, but is vital for understanding the uncertainty in the graph structure itself. To achieve robust inference we need to account for the structure uncertainty in analyses further downstream (Kuipers et al., 2018), for example for causal interpretations and in the estimation of intervention effects (Moffa et al., 2017).

## Acknowledgements

The authors would like to thank Markus Kalisch and Niko Beerenwinkel for useful comments and discussions.

Parent nodes	Node score	Banned parents	Summed node score
$\emptyset$	$S_0^i = S(X_i, \{\emptyset\} \mid D)$	$\emptyset$	$\Sigma_7^i = \sum_{j=0}^7 S_j^i$
$h_1^i$	$S_1^i = S(X_i, \{h_1^i\} \mid D)$	$h_1^i$	$\Sigma_6^i = S_0^i + S_2^i + S_4^i + S_6^i$
$h_2^i$	$S_2^i = S(X_i, \{h_2^i\} \mid D)$	$h_2^i$	$\Sigma_5^i = S_0^i + S_1^i + S_4^i + S_5^i$
$h_3^i$	$S_4^i = S(X_i, \{h_3^i\} \mid D)$	$h_3^i$	$\Sigma_3^i = S_0^i + S_1^i + S_2^i + S_3^i$
$h_1^i, h_2^i$	$S_3^i = S(X_i, \{h_1^i, h_2^i\} \mid D)$	$h_1^i, h_2^i$	$\Sigma_4^i = S_0^i + S_4^i$
$h_1^i, h_3^i$	$S_5^i = S(X_i, \{h_1^i, h_3^i\} \mid D)$	$h_1^i, h_3^i$	$\Sigma_2^i = S_0^i + S_2^i$
$h_2^i, h_3^i$	$S_6^i = S(X_i, \{h_2^i, h_3^i\} \mid D)$	$h_2^i, h_3^i$	$\Sigma_1^i = S_0^i + S_1^i$
$h_1^i, h_2^i, h_3^i$	$S_7^i = S(X_i, \{h_1^i, h_2^i, h_3^i\} \mid D)$	$h_1^i, h_2^i, h_3^i$	$\Sigma_0^i = S_0^i$

Table S1: An example score table of a node with 3 permissible parents in the search space (left). For each possible list of excluded parents, we also create a second table (right) containing the sum of scores of all subsets of remaining parents.

## Supplementary Material

### Appendix A. Algorithmic details for computing summed score tables

Given the scores of all permissible parent sets of a node (Table S1, left), we detail how to compute the summed score (Table S1, right). The first column indicates which nodes are banned as parents and the second column reports the sum of scores over all parent subsets excluding those nodes. For the indexing of the sums we negate the indicator function:

$$\bar{f}(\mathbf{Z}) = \sum_{j=1}^K I(h_j^i \notin \mathbf{Z}) 2^{j-1} = 2^K - f(\mathbf{Z}) - 1 \quad (28)$$

#### A.1 Power set representation

A Hasse diagram (Figure S1) visualises the power set of the permissible parents with layers ranked by the size of the parent subsets, and helps develop a strategy to efficiently evaluate the partial sums over parent subsets. Directed edges indicate the addition of another parent to each subset, while the corresponding scores of each parent subset are attached to the nodes in Figure S1. The advantage of the Hasse representation is that each element in the summed score table (right of Table S1) is the sum of the scores of a node and all its ancestors in the network. Power set representations have also been previously used for Bayesian network inference, for example by Koivisto and Sood (2004) to sum over orders.

#### A.2 Score propagation

To actually perform the sums we utilise the separation of the power set into  $(K+1)$  layers of differently sized parent subsets and implement Algorithm S1. The partial sums at each layer are propagated to their children in the network. To avoid overcounting contributions from ancestors which are propagated along all  $d!$  paths connecting nodes  $d$  layers apart, we divide

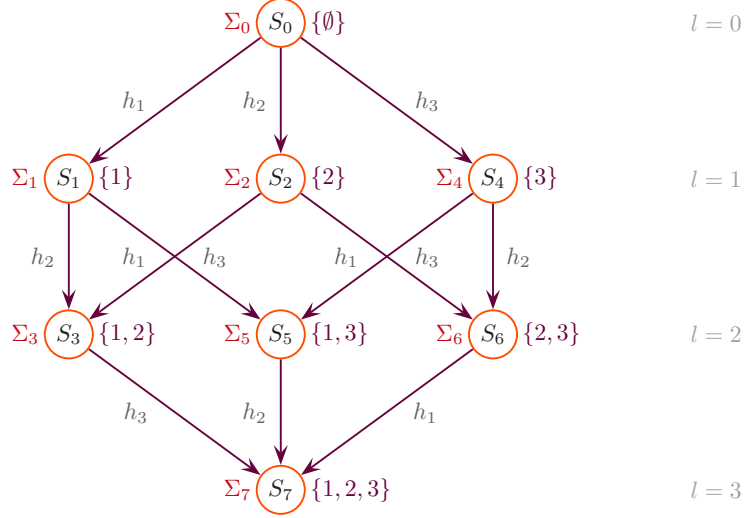


Figure S1: In the Hasse diagram the permissible parent subsets can be arranged by their size and connected as a network where parents are added along each directed edge. The subsets are indicated on the right side of each node. Inside the nodes of the network are the scores of that particular parent subset. To the left of each node we place the sum of scores of that node and all its ancestors in the network. This sum encompass all possible subsets which exclude any members of the complement.

by the corresponding factorials to obtain the required sums. This division is separated over the layers by dividing by one of the factorial terms each time. For each end layer there are a different number of ancestral paths to the nodes in previous layers leading to different correction factors, so we need to repeat the propagation  $K$  times. Building the summed score table for each variable has a complexity of  $O(K^2 2^K)$ : during each propagation, the value at each of the  $2^K$  elements of the power set is created by adding its starting value with the values of its parents of which there can be at most  $K$  giving a complexity of  $O(K 2^K)$ , while the propagation is repeated  $K$  times.

### A.3 MAP DAG targetting

When assigning the score of each order to be the maximum score of DAGs in the order, we do not need to worry about the overcounting and can propagate only once in  $O(K 2^K)$ , see Algorithm S2.

### A.4 Restricted sums

For the partition based sampling, we need to ensure that nodes receive at least one edge from the adjacent partition element. For the example with 3 permissible parents, there are the 8 values calculated in Table S1 where there was no restriction on enforcing the presence of a member of the needed parent subset (which we regard as the empty set).

---

**Algorithm S1** Obtain the sum of scores of all parent subsets excluding banned nodes
 

---

**Input** The power set network of the  $K$  permissible parents of variable  $i$   
**Input** The table of scores of each parent subset  $S_j^i$ ,  $j = 0, \dots, (2^K - 1)$   
 Label the network nodes  $Y_{f(\mathbf{Z})}$  for each  $\mathbf{Z}$  in the power set  
 Initialise the node at layer 0:  $\Sigma_0^i = Y_0 = S_0^i$   
**for**  $l = 1$  to  $K$  **do** ▷ layer number  
     **for**  $m = 0$  to  $(l - 1)$  **do**  
         Initialise the value of all nodes in layer  $(m + 1)$ :  
         **for all**  $\{j \in \text{layer } (m + 1)\}$  **do**  
              $Y_j = S_j^i$   
         **end for**  
         Add the value of nodes  $Y_j$  at layer  $m$ , divided by  $(l - m)$ ,  
         to all children in the power set network at layer  $(m + 1)$ :  
         **for all**  $\{j \in \text{layer } m\}$  **do**  
             **for all**  $\{j' \mid Y_{j'} \text{ child of } Y_j\}$  **do**  
                  $Y_{j'} = Y_{j'} + \frac{Y_j}{(l - m)}$  ▷ division accounts for overcounting  
             **end for**  
         **end for**  
     **end for**  
     Read off sum scores at layer  $l$ :  
     **for all**  $\{j \in \text{layer } l\}$  **do**  
          $\Sigma_j^i = Y_j$   
     **end for**  
**end for**  
**return** Table of summed scores:  $\Sigma_j^i$ ,  $j = 0, \dots, (2^K - 1)$

---



---

**Algorithm S2** Obtain the maximal score among all parent subsets excluding banned nodes
 

---

**Input** The power set network of the  $K$  permissible parents of variable  $i$   
**Input** The table of scores of each parent subset  $S_j^i$ ,  $j = 0, \dots, (2^K - 1)$   
 Label the network nodes  $Y_{f(\mathbf{Z})}$  for each  $\mathbf{Z}$  in the power set  
 Initialise all nodes:  $Y_j = S_j^i$ ,  $j = 0, \dots, (2^K - 1)$   
**for**  $l = 1$  to  $K$  **do** ▷ layer number  
     Replace the value of nodes  $Y_j$  at layer  $l$  by the maximum of itself  
     and all its parents in the power set network at layer  $(l - 1)$ :  
     **for all**  $\{j \in \text{layer } l\}$  **do**  
         **for all**  $\{j' \mid Y_{j'} \text{ parent of } Y_j\}$  **do**  
              $Y_j = \max(Y_j, Y_{j'})$   
         **end for**  
     **end for**  
**end for**  
**return** Table of maximal scores:  $M_j^i = Y_j$ ,  $j = 0, \dots, (2^K - 1)$

---

Additionally there are the 19 combinations in Table S2 where we index the sums with the

Banned parents	Needed parents	Summed node score
$\emptyset$	$h_1^i$	$\tilde{\Sigma}_2^i = S_1^i + S_3^i + S_5^i + S_7^i$
$\emptyset$	$h_2^i$	$\tilde{\Sigma}_6^i = S_2^i + S_3^i + S_6^i + S_7^i$
$\emptyset$	$h_3^i$	$\tilde{\Sigma}_{18}^i = S_4^i + S_5^i + S_6^i + S_7^i$
$\emptyset$	$h_1^i, h_2^i$	$\tilde{\Sigma}_8^i = S_1^i + S_2^i + S_3^i + S_5^i + S_6^i + S_7^i$
$\emptyset$	$h_1^i, h_3^i$	$\tilde{\Sigma}_{20}^i = S_1^i + S_3^i + S_4^i + S_5^i + S_6^i + S_7^i$
$\emptyset$	$h_2^i, h_3^i$	$\tilde{\Sigma}_{24}^i = S_2^i + S_3^i + S_4^i + S_5^i + S_6^i + S_7^i$
$\emptyset$	$h_1^i, h_2^i, h_3^i$	$\tilde{\Sigma}_{26}^i = S_1^i + S_2^i + S_3^i + S_4^i + S_5^i + S_6^i + S_7^i$
$h_1^i$	$h_2^i$	$\tilde{\Sigma}_7^i = S_2^i + S_6^i$
$h_1^i$	$h_3^i$	$\tilde{\Sigma}_{19}^i = S_4^i + S_6^i$
$h_1^i$	$h_2^i, h_3^i$	$\tilde{\Sigma}_{25}^i = S_2^i + S_4^i + S_6^i$
$h_2^i$	$h_1^i$	$\tilde{\Sigma}_5^i = S_1^i + S_5^i$
$h_2^i$	$h_3^i$	$\tilde{\Sigma}_{21}^i = S_4^i + S_5^i$
$h_2^i$	$h_1^i, h_3^i$	$\tilde{\Sigma}_{23}^i = S_1^i + S_4^i + S_5^i$
$h_3^i$	$h_1^i$	$\tilde{\Sigma}_{11}^i = S_1^i + S_3^i$
$h_3^i$	$h_2^i$	$\tilde{\Sigma}_{15}^i = S_2^i + S_3^i$
$h_3^i$	$h_1^i, h_2^i$	$\tilde{\Sigma}_{17}^i = S_1^i + S_2^i + S_3^i$
$h_1^i, h_2^i$	$h_3^i$	$\tilde{\Sigma}_{22}^i = S_4^i$
$h_1^i, h_3^i$	$h_2^i$	$\tilde{\Sigma}_{16}^i = S_2^i$
$h_2^i, h_3^i$	$h_1^i$	$\tilde{\Sigma}_{14}^i = S_1^i$

Table S2: An example sum score table for each possible list of excluded parents, where at least one member of the needed parents subset must be included.

ternary mapping of Eq. (25). We also define the mapping back to the banned parent set

$$\tilde{g}(j) = \mathbf{Z} \mid g(\mathbf{Z}, \mathbf{W}) = j \quad (29)$$

Again we build a network representation of the possibilities by replicating each node in the power set representation according to the number of choices of possible needed parent subsets in the complement of the banned parent subsets. We rank the nodes by the size of the banned node subsets as in Figure S2, and assign to the nodes the score corresponding to the complement of the banned node subset. The connections in the network represent either removing an element from the banned parent subset, or moving it to the needed parent subset. For any  $j$  such that  $\mathbf{h}_j^i$  is in the banned parent subset there is then an edge to the node indexed by  $3^{j-1}$  more and the node indexed by  $3^{j-1}$  less using the ternary mapping of Eq. (25).



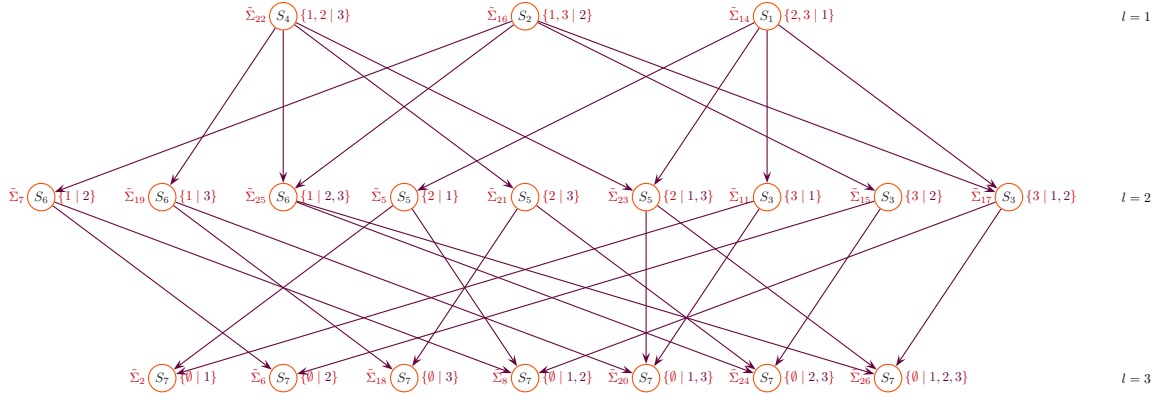


Figure S2: The banned parent subsets can be arranged by their size and expanded to include all needed parent subsets in the complement. Inside the nodes of the network are the scores of the complement of the banned parent subset, and both the banned and needed parents subsets are indicated on the side of each node. The nodes are connected as a network where parents are deleted from the banned parent subsets or moved into the needed parent subsets. The sum of all scores which do not involve certain banned parents but do include at least one member of the needed parent subset is simply the sum of scores associated with a node and all its ancestors in the network.

The sums in Table S2 are the sums of the scores of each node in the network in Figure S2 and its ancestors. To compute these sums efficiently we again propagate through the network using Algorithm S3 whose complexity is  $O(K^2 3^K)$ .

## Appendix B. Simulation studies

To examine the performance and convergence of our method, we performed a simulation study for 4 network sizes  $n \in \{20, 80, 140, 200\}$  and 2 sample sizes  $N \in \{2n, 10n\}$ . For each combination of network and sample sizes, 100 random graphs and corresponding data were generated using the functions `randomDAG` and `rmvDAG` from the `pcalg` package. The strengths of the edges were in the range  $[0.4, 2]$ . The edge probability parameter was set to  $\frac{4}{n}$ , so that the average number of edges in the DAG equals  $2(n-1)$  and the average parent set size per node is just under 2. Although the average number of parents is around 2, the determining factor for the run time is the maximal number of parents. With 20 nodes the maximal number of parents is 6 on average, rising to 8 on average with 80 nodes (with more than 5% of cases having 10 parents or more) and further increases for larger networks.

Methods which impose a hard limit on the number of parents, as is the case with leading score-based schemes (Friedman and Koller, 2003; Teyssier and Koller, 2005; Grzegorzcyk and Husmeier, 2008; Kuipers and Moffa, 2017) including ILP solvers (Cussens, 2011; Cussens et al., 2017), scale in complexity as  $O(n^{K+1})$  and simply do not scale to our simulation setting. Order-based schemes for MAP DAG discovery, can prune the sets of permissible

---

**Algorithm S3** Obtain the sum of scores of all parent sets excluding all banned nodes but including at least one member of needed nodes

---

**Input** The network of the banned and needed parent subsets of variable  $i$  from the  $K$  permissible parents

**Input** The table of scores of each parent set  $S_j^i$ ,  $j = 0, \dots, (2^K - 1)$

**Input** The table of summed scores for each banned parent subset  $\Sigma_j^i$ ,  $j = 0, \dots, (2^K - 1)$

Label the network nodes  $Y_{g(\mathbf{Z}, \mathbf{W})}$

Initialise the restricted summed scores for empty needed nodes:

**for**  $j = 0$  to  $(2^K - 1)$  **do**

$\tilde{\Sigma}_{g(f^{-1}(j), \emptyset)}^i = \Sigma_j^i$

**end for**

Initialise the nodes at layer 1:

**for all**  $\{j \in \text{layer } 1\}$  **do**

$\tilde{\Sigma}_j^i = Y_j = S_{\tilde{f}(\tilde{g}(j))}^i$

**end for**

**for**  $l = 2$  to  $K$  **do**

**for**  $m = 1$  to  $(l - 1)$  **do**

Initialise the value of all nodes in layer  $(m + 1)$ :

**for all**  $\{j \in \text{layer } (m + 1)\}$  **do**

$Y_j = S_{\tilde{f}(\tilde{g}(j))}^i$

**end for**

Add the value of nodes  $Y_j$  at layer  $m$ , divided by  $(l - m)$ , to all children in the network at layer  $(m + 1)$ :

**for all**  $\{j \in \text{layer } m\}$  **do**

**for all**  $\{j' \mid Y_{j'} \text{ child of } Y_j\}$  **do**

$Y_{j'} = Y_{j'} + \frac{Y_j}{(l - m)}$

**end for**

**end for**

**end for**

Read off restricted sum scores at layer  $l$ :

**for all**  $\{j \in \text{layer } l\}$  **do**

$\tilde{\Sigma}_j^i = Y_j$

**end for**

**end for**

**return** Table of restricted summed scores:  $\tilde{\Sigma}_j^i$ ,  $j = 0, \dots, (2^K - 1)$

---

parents to reduce this computational burden (Friedman and Koller, 2003; Teyssier and Koller, 2005). A recent implementation (Scanagatta et al., 2015) can only handle categorical variables, so we compare to that approach in Section B.5.

For continuous data we therefore compare only to GES (Chickering, 2002a), a greedy structure-based search, and the PC algorithm (Spirtes et al., 2000), a constraint-based method. The hybrid approach of Tsamardinos et al. (2006) of a greedy structure search in

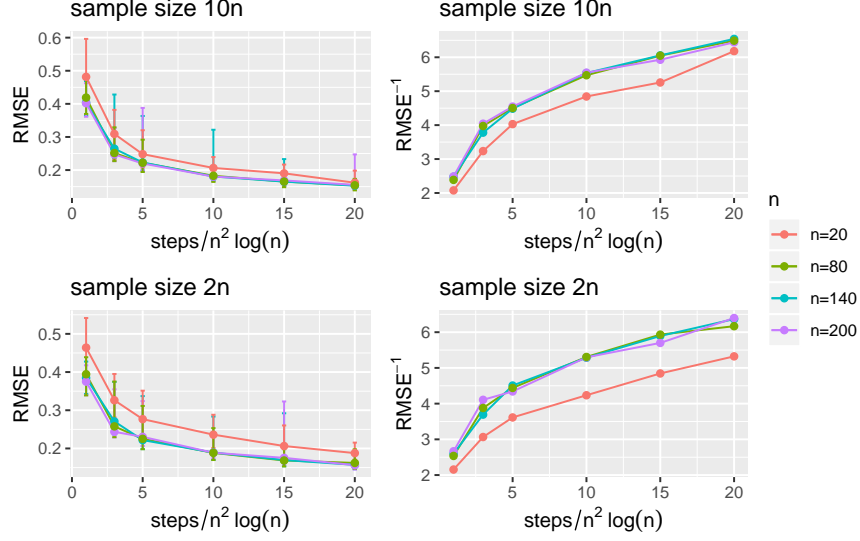


Figure S3: The root mean square error (RMSE) between edge probabilities from pairs of different runs for each simulation as the size of the network increases. The runs are those from Figure S3 where the correlation  $\rho^2$  was displayed.

a constraint-based skeleton performs very similarly to the PC algorithm and is not included in the comparisons.

### B.1 Skeleton inference

To assess the performance we first considered the number of true positives (TP) and false positives (FP) in the undirected skeletons of the networks inferred and scaled them by the number of edges (P) in the true DAG

$$\text{TPR} = \frac{\text{TP}}{P} \quad \text{FPR}_n = \frac{\text{FP}}{P} \quad (30)$$

We computed the median TPR along with the first and third quartiles and plotted (Figures 4 and S4) against the median  $\text{FPR}_n$  over the 100 realisations for our MCMC scheme for two search spaces: the initial search space defined by the PC algorithm skeleton, and expanded to include an additional parent; and the final search space which is improved iteratively until it contains the MAP DAG discovered. Also plotted are the results from GES (Chickering, 2002a) and the PC algorithm using Fisher's  $z$  test for conditional independence (Spirtes et al., 2000; Kalisch et al., 2012). The range of discrimination thresholds for plotting points in the ROC curves were:

- penalisation parameter  $\frac{\lambda}{\log(N)} \in \{1, 2, 5, 7, 9, 11, 15, 25\}$  for GES
- significance level  $\alpha \in \{0.01, 0.05, 0.1, 0.2, 0.35, 0.45\}$  for the PC algorithm (the highest threshold may result in too many false positives to display in the plots)

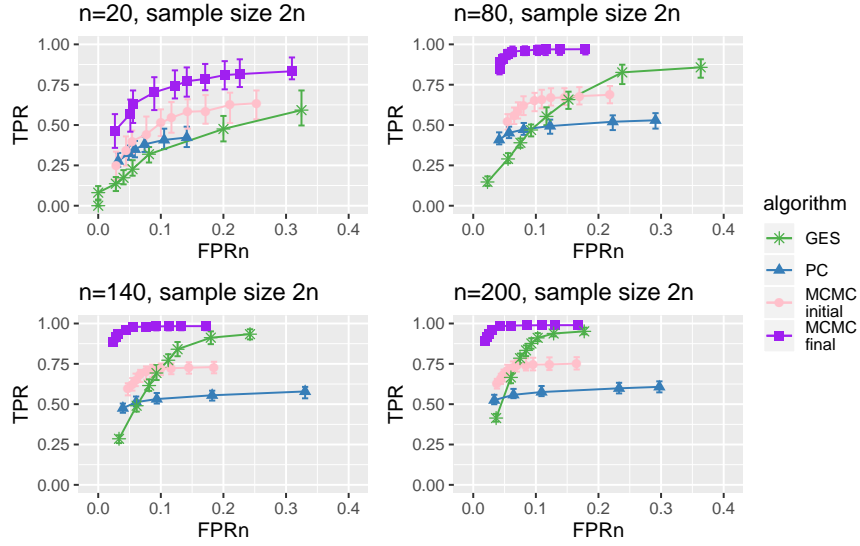


Figure S4: The performance in recovering the underlying DAG skeleton. The graph is as Figure 4 but with a smaller sample size of  $N = 2n$ .

- posterior probability  $\rho \in \{0.2, 0.3, 0.4, 0.5, 0.6, 0.7, 0.8, 0.9, 0.95, 0.99\}$  for MCMC

With the initial search space, we see a distinct improvement with our MCMC scheme (pink circles in Figures 4 and S4), while when we improve the search space iteratively we observe a strong advantage over the alternative methods (purple squares in Figures 4 and S4) and approach perfect recovery of the skeleton for the larger sample size (Figure 4).

In the simulations, increasing the significance level of the conditional independence tests of the PC algorithm does not really improve the recovery of true edges, while the additional false positives start to dramatically increase the algorithm’s runtime.

## B.2 Iterative steps

To explore how the iterative search leads to an improvement in performance we keep track of the highest scoring DAG uncovered at each iteration, and used to update the core search space for the next iteration. In Figure S5, we overlay these intermediate results on the MCMC lines of Figure 4. Each iteration, and especially the earlier ones leads to an improvement in the search space allowing the MCMC search to find better DAGs which were previously excluded. Finally, utilising the posterior probability of edges in the sample from the final search space, we can remove some of the false positive edges in the point estimate of the highest scoring DAG uncovered.

## B.3 Direction inference

Along with inferring the undirected skeleton, we also assess the performance in recovering the correct directions and compute the structural Hamming distance (SHD) between the true generating DAG and those inferred by the different methods. In all cases we convert to

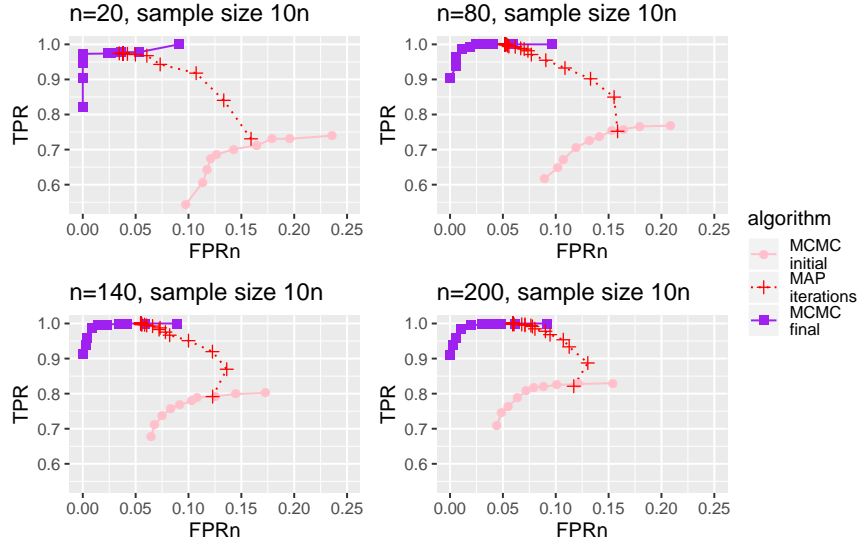


Figure S5: How the iterative search improves performance, using the setting of Figure 4 as an example. Starting from the search skeleton defined by the PC algorithm, expanded to include an possible additional parent (pink circles) we plot the highest scoring DAG discovered in that search space and during subsequent iterations (red plusses). When no better DAG is discovered, sampling from the final search space provides the purple squares.

CPDAGs before computing the distances. For GES we used the penalisation  $\lambda = 2 \log(N)$  while for the PC algorithm we used a significance level of  $\alpha = 0.05$ . To condense the sample of DAGs from our MCMC schemes to a single graph, we converted the sample to CPDAGs and retained edges occurring with a posterior probability greater than 0.5. The result for targeting a MAP DAG correspond to the highest scoring DAG discovered in the final search space, again transformed into a CPDAG.

The results (Figures S6 and S7) again show a strong improvement of our MCMC approach over the alternative algorithms. Sampling and performing Bayesian model averaging also offers a consistent advantage over taking a MAP point estimate.

#### B.4 Other DAG types

For the same settings as in Figure 4, of graphs of size  $n \in \{20, 80, 140, 200\}$  with a sample size of  $N = 10n$  and an average parent set size of 2, which we denote by  $\nu = 2$ , we sample Erdős-Rényi DAGs instead using that option in the `randDAG` function of the `pcalg` package. We observe (Figure S8) a slight worsening in the GES results and a slight improvement in the PC algorithm results (compared to the previous simulation, Figure 4), and again a strong advantage for our MCMC approach.

For Barabási-Albert scale-free or power-law DAGs, again with an average of 2 parents (Figure S9), there is a further decrease in the performance of GES and a slight increase in false positives of our MCMC scheme. Nonetheless, it still recovers almost all true positives,

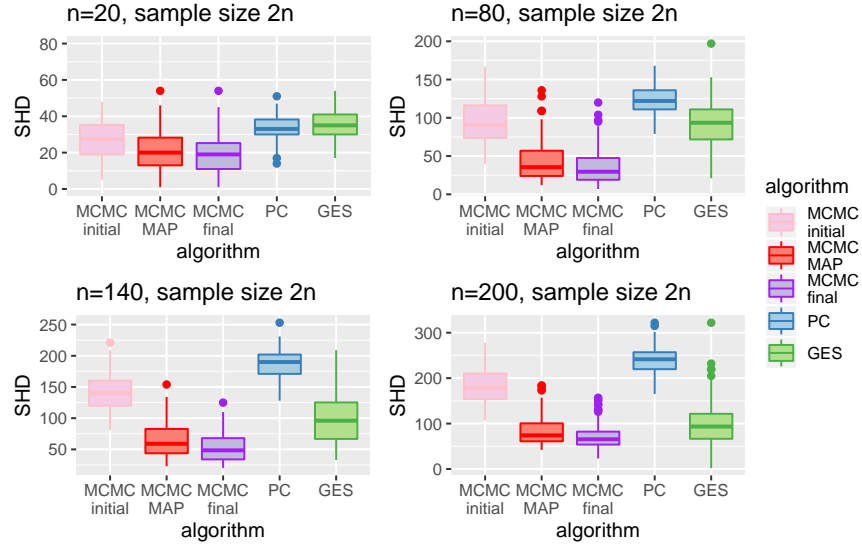


Figure S6: The performance in recovering the CPDAG measured by the structural Hamming distance (SHD). We compare the performance of our MCMC sampler (purple) and the highest scoring (MAP) DAG (red) from the final search space to the PC algorithm (blue) and GES (green), along with the MCMC sampler from a search space of the the PC algorithm skeleton expanded to include one additional parent (pink).

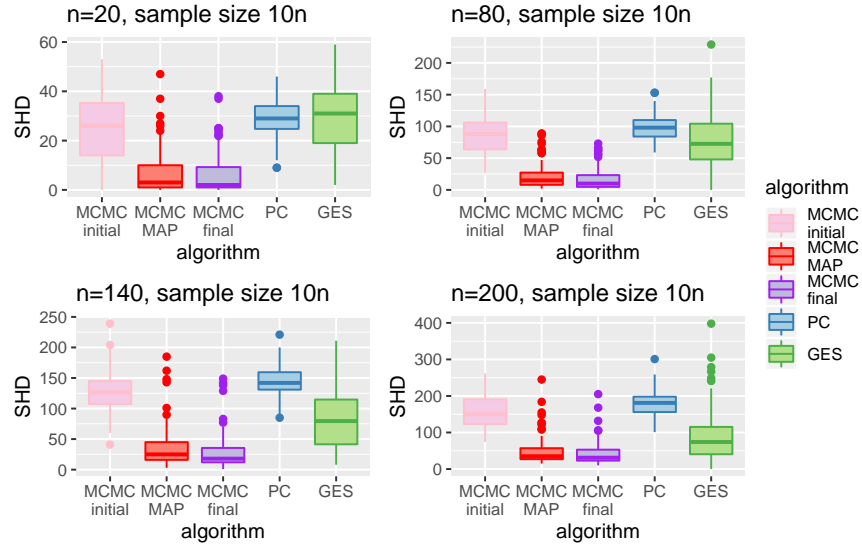


Figure S7: The performance in recovering the CPDAG. The graph is as Figure S6 but with a smaller sample size of  $N = 2n$ .

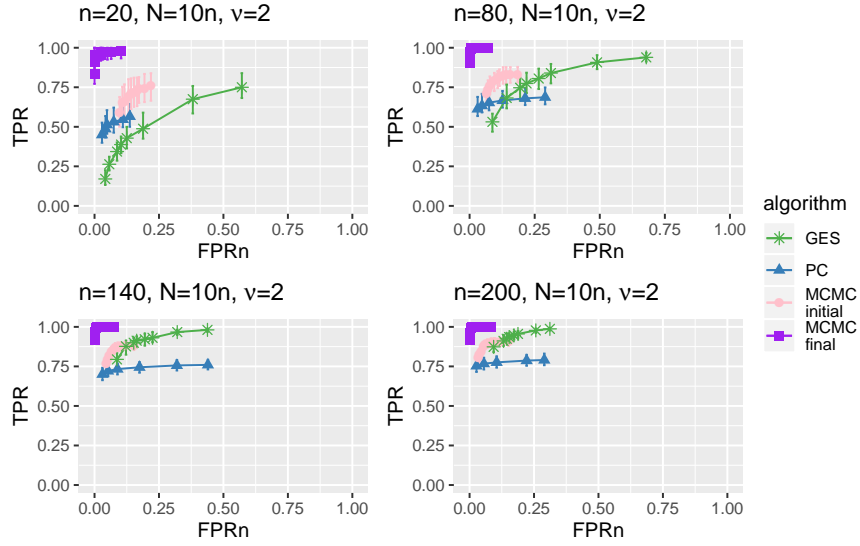


Figure S8: The performance in recovering the underlying DAG skeleton for Erdős-Rényi DAGs with 2 parents on average. We compare the performance of our MCMC scheme (purple squares) on its final search space, to the PC algorithm (blue triangles) and GES (green stars).

unlike the alternatives. By sparsifying the graphs and setting the average number of parents to 1 instead, our MCMC scheme performs very well, the PC algorithm captures most true edges, but GES obtains essentially perfect performance (Figure S10).

Increasing the density instead to have an average of 3 parents per node, and having a network made up of two Erdős-Rényi islands with an interconnectivity parameter of 0.1 (Figure S11), we observe that our MCMC scheme has a marked increase in false positive edges (up to around 40% of the number of true positives) and that we also miss out on some true edges. We can track this loss of performance down to the fact that the final search space does not include the true DAG, for when we artificially add it to the search space (grey diamonds, Figure S11) we again have near perfect performance for larger networks. Modifications to improve finding the best search space for our MCMC sampler could therefore significantly improve its performance for denser networks.

Although our MCMC scheme does miss out on some true edges, the PC algorithm struggle to find even half of them while GES finds some more, but at the cost of a large number of false positives. Both alternatives perform substantially worse than MCMC.

In terms of run times, the final MCMC sampling is roughly an order of magnitude slower than finding the initial search space with the PC algorithm, but the bulk of the time is in the iterative steps to find the final search space, which can be roughly an order of magnitude slower again (Figure S12). As the final search space can have a strong effect on the performance for denser networks (Figure S11), improvements in the speed of finding it could also be beneficial. The actual run times of the full algorithm averages around 10 seconds for 20 nodes, around 10 minutes for 80 nodes, and up to a few hours for 200 nodes.

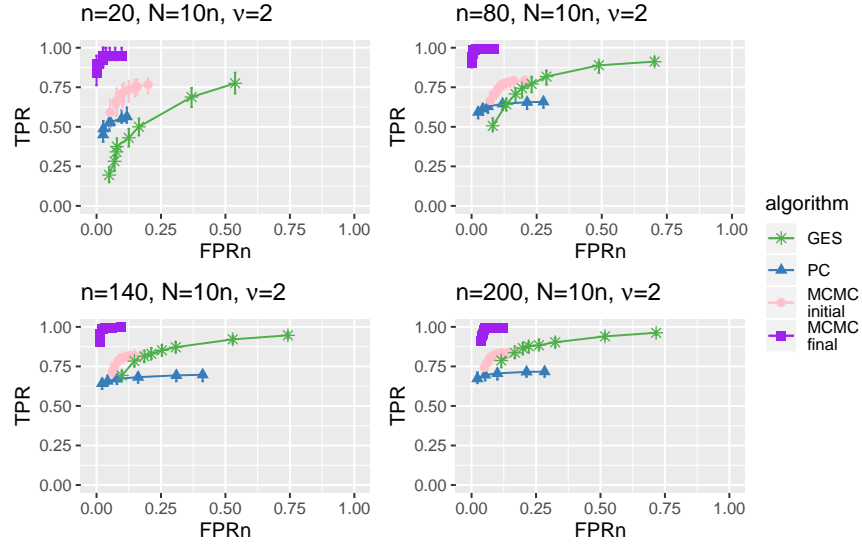


Figure S9: The performance in recovering the underlying DAG skeleton for Barabási-Albert DAGs with 2 parents on average.

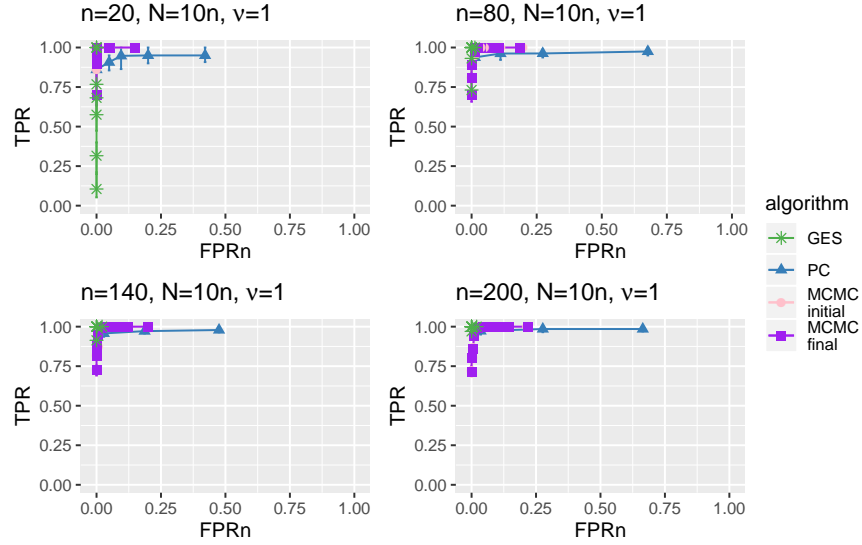


Figure S10: The performance in recovering the underlying DAG skeleton for Barabási-Albert DAGs with 1 parent on average.

## B.5 Categorical simulations

To compare to the order-based search implemented in **r.blip** (Scanagatta et al., 2015), we had to simulate categorical data. First we considered the ANDES network with  $n = 223$



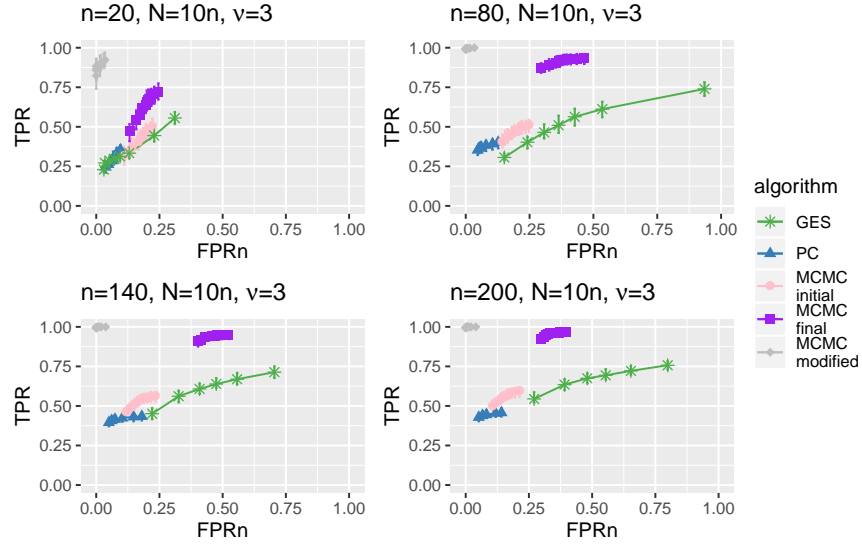


Figure S11: The performance in recovering the underlying DAG skeleton for a pair of Erdős-Rényi islands with an interconnectivity coefficient of 0.1 and 3 parents on average. The MCMC performance on a search space artificially including the true DAG is illustrated with grey diamonds.

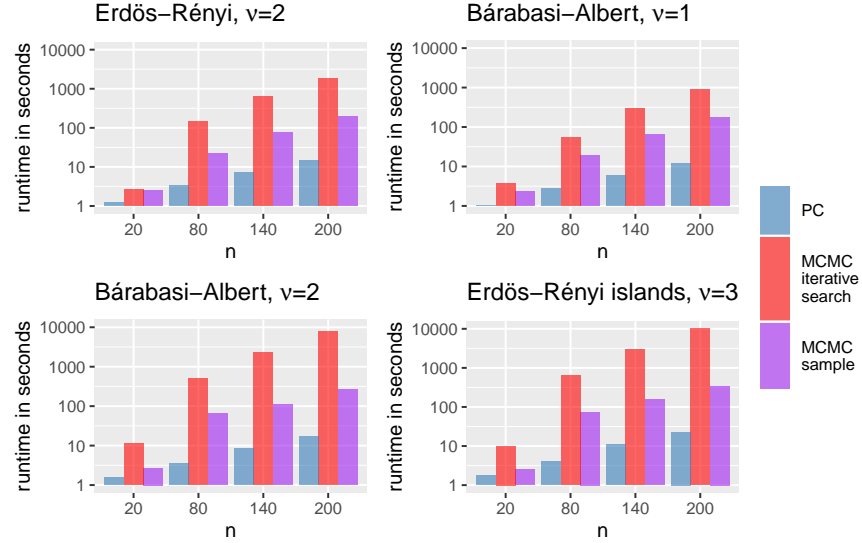


Figure S12: The average runtimes of finding the initial search space with the PC algorithm (blue), iteratively improving the search space (red) and the final MCMC sampling (purple) for the four different network settings.

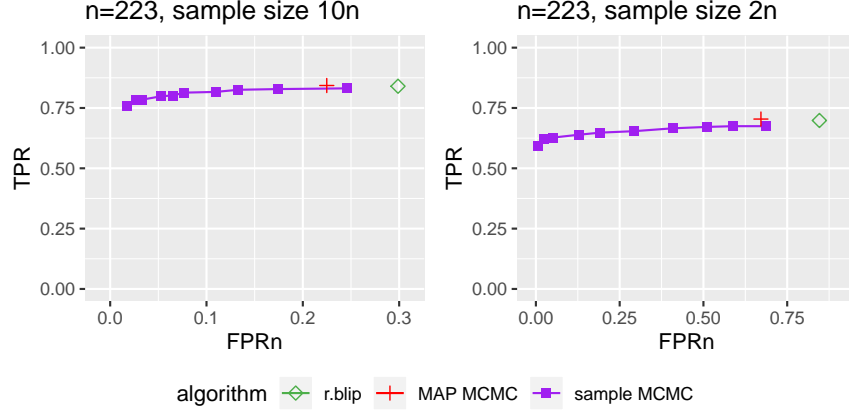


Figure S13: The accuracy in learning the ANDES network. We compare the performance of **r.blip** to the MAP DAG search of **BiDAG** and its posterior sampling.

nodes for which we generated random samples (with the **bnlearn** package; Scutari, 2010) for two sample sizes  $N = 2n$  and  $N = 10n$ . Fixing the score parameters to those in **r.blip** and using the same runtime (1500 seconds) we find similar high scores (slightly higher for **BiDAG** for  $N = 2n$ : -42844.62 against -42856.39; and slightly lower for  $N = 10n$ : -209833.8 against -209811.9). Irrespective of the score, we find a much better structure with **BiDAG** with notably fewer false positive edges (Figure S13). Moreover, by accounting for the uncertainty in the edges and considering a posterior sample as opposed to a point estimate, we can drastically reduce the number of false positive edges while retaining true edges.

A similar pattern is repeated in a larger scale simulation of 100 binary power-law networks (with 1 parent on average and a maximum of 5). In terms of score, we routinely find higher scoring graphs at the larger sample size, but mostly lower scores at the lower sample size (Figure S14). The higher score at the lower sample size is however driven by false positives and does not lead to a more accurate graph structure (Figure S15). Indeed running **r.blip** for longer times, while increasing the score on average, solely increases the false positive rate with no improvement in finding true edges. Although the highest scoring DAGs returned by **BiDAG** is more accurate than those of **r.blip**, the real advantage comes again by sampling and using a posterior threshold to remove false positive edges, which heavily improves the accuracy in network inference.

## Appendix C. Categorical data

For categorical data, we employ the BDe score (Heckerman and Geiger, 1995). For ease of presentation, we details the binary case here. For any node  $X_i$ , its contribution to the score involves computing the number of times  $X_i$  takes the value 1, or the value 0, for each of the  $2^K$  possible configurations of its  $K$  parents  $\mathbf{Pa}_i$ . All the parents for each of the  $N$  observations must be run through in a complexity of  $O(KN)$ . As there is a parameter associated with each of the  $2^K$  parent configurations, we assume  $N \gg 2^K$ . Building the

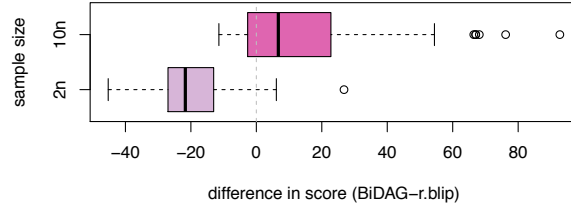


Figure S14: The relative log scores of the highest scoring DAG returned by **r.blip** and by **BiDAG** for random networks of  $n = 100$  nodes. The runtime for **r.blip** was fixed to 240 seconds, while **BiDAG** had an average time of 150 seconds.

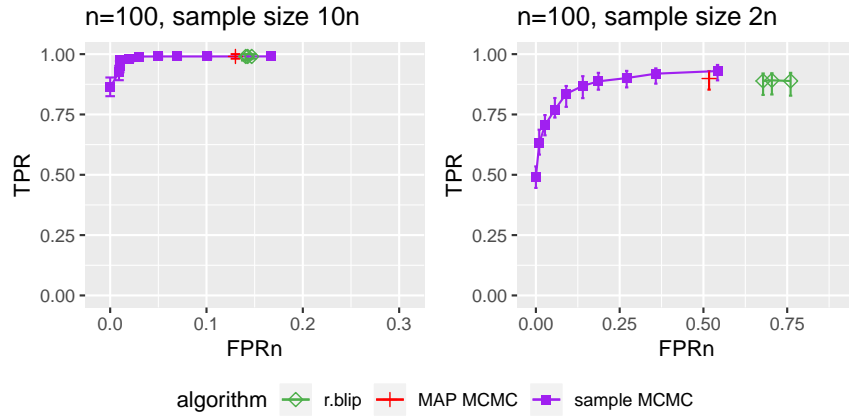


Figure S15: The accuracy in learning random networks with  $n = 100$  nodes. We compare the performance of **r.blip** to the MAP DAG search of **BiDAG** and its posterior sampling. The 3 points (left to right) for **r.blip** corresponds to runtimes of 60, 120 and 240 seconds, while **BiDAG** had an average time of 150 seconds for MAP discovery, and 30 seconds for sampling.

score table of node  $X_i$  by naively running through all parent configurations would take  $O(K2^K N) \gg O(K4^K)$ .

However the parent configurations are connected via the poset structure of Figure S1, so we can build the score table more efficiently by only looking at the raw data once. For the BDe score, for the case when all  $K$  parents are present we build the vectors  $\mathbf{N}_1^i(\mathbf{h}^i)$  and  $\mathbf{N}_0^i(\mathbf{h}^i)$  whose  $2^K$  elements count the number of times  $X_i$  takes the value 1 and 0 for each parent state, in time  $O(KN)$ . We employ a binary mapping of the parent states to elements of the vectors using

$$\sum_{j=1}^{|\mathbf{Z}|} I(Z_j = 1)2^{j-1} \quad (31)$$

where for the full set of parents,  $\mathbf{Z} = \mathbf{h}^i$ . When we remove one of the parents to compute the score table entry at layer  $(K - 1)$  in the poset of Figure S1 we simply combine elements

---

**Algorithm S4** Obtain the scores of all parent sets for binary data
 

---

**Input** The power set network of the  $K$  permissible parents of variable  $i$   
**Input** The count vectors of the full parent set  $\mathbf{N}_{\{1,0\}}^i(\mathbf{h}^i)$   
 Label the network nodes  $Y_{f(\mathbf{Z})}$  for each  $\mathbf{Z}$  in the power set  
 Compute the score  $S_{2^K-1}^i$  at layer  $K$  from the  $\mathbf{N}_{\{1,0\}}^i(\mathbf{h}^i)$   $\triangleright$  Eq. (34)  
**for**  $l = K - 1$  to  $0$  **do**  $\triangleright$  layer number  
     **for all**  $\{j \in \text{layer } l\}$  **do**  
         Choose any child in the network  
         Compute  $\mathbf{N}_{\{1,0\}}^i(f^{-1}(j))$  from the child  $\triangleright$  Eq. (32)  
         Compute  $S_j^i$  from the  $\mathbf{N}_{\{1,0\}}^i(f^{-1}(j))$   $\triangleright$  Eq. (34)  
     **end for**  
**end for**  
**return** Table of scores:  $S_j^i, j = 0, \dots, (2^K - 1)$

---

of the vector  $\mathbf{N}_{\{1,0\}}^i$  where the removed parent takes the value 0 with the corresponding elements where it takes the value 1. In general we can create the vectors at each level from any connected at a higher level with

$$\mathbf{N}_{\{1,0\}}^i(\mathbf{Z} \setminus \mathbf{Z}_j)[t] = \mathbf{N}_{\{1,0\}}^i(\mathbf{Z})[v(t, j)] + \mathbf{N}_{\{1,0\}}^i(\mathbf{Z})[v(t, j) + 2^{j-1}] \quad (32)$$

where the square brackets indicate the elements of the vectors and we employ the mapping

$$v(t, j) = t + \left( \left\lceil \frac{t}{2^{j-1}} \right\rceil - 1 \right) 2^{j-1} \quad (33)$$

From the pair of vectors for any set of permissible parent nodes  $\mathbf{N}_{\{1,0\}}^i(\mathbf{Z})$  we can compute the entry in the score table according to the BDe score (Heckerman and Geiger, 1995)

$$S_{f(\mathbf{Z})}^i = \sum_{t=1}^{2^m} \frac{\Gamma(\frac{\chi}{2^m})}{\Gamma(\frac{\chi}{2^{m+1}}) \Gamma(\frac{\chi}{2^{m+1}})} \frac{\Gamma(\mathbf{N}_1^i(\mathbf{Z})[t] + \frac{\chi}{2^{m+1}}) \Gamma(\mathbf{N}_0^i(\mathbf{Z})[t] + \frac{\chi}{2^{m+1}})}{\Gamma(\mathbf{N}_1^i(\mathbf{Z})[t] + \mathbf{N}_0^i(\mathbf{Z})[t] + \frac{\chi}{2^m})} \quad (34)$$

with  $m = |\mathbf{Z}|$  and  $\chi$  the hyperparameters of the beta distributions which correspond to pseudocounts in the score.

Repeating the creation of the count vectors and computation of the score by moving up the layers in the poset of Figure S1, as summarised in Algorithm S4, we efficiently build the score table for each node in the data. For each term at layer  $l$  we look at vectors from the layer above of size  $2^{l+1}$  so that filling out the score tables takes  $O(3^K)$ . Combining with the initial step leads to an overall complexity of  $O(\max\{KN, 3^K\})$  which is a significant improvement on the naive implementation of  $O(\max\{K2^K N, K4^K\})$ .

For categorical data, the same approach is followed, although with mixed radix indexing for different sized categories rather than the simple binary mapping discussed above. With more possible states, the complexity also increases. For example if all categories have  $C$  levels, the complexity is  $O((C+1)^K)$ .

## References

- S. A. Andersson, D. Madigan, and M. D. Perlman. A characterization of Markov equivalence classes for acyclic digraphs. *Annals of Statistics*, 25:505–541, 1997.
- W. Buntine. Theory refinement on Bayesian networks. In *Seventh Conference on Uncertainty in Artificial Intelligence*, pages 52–60, 1991.
- D. M. Chickering. Optimal structure identification with greedy search. *Journal of Machine Learning Research*, 3:507–554, 2002a.
- D. M. Chickering. Learning equivalence classes of Bayesian-network structures. *Journal of Machine Learning Research*, 2:445–498, 2002b.
- D. Colombo and M. H. Maathuis. Order-independent constraint-based causal structure learning. *Journal of Machine Learning Research*, 15:3741–3782, 2014.
- G. Consonni and L. L. Rocca. Objective Bayes factors for Gaussian directed acyclic graphical models. *Scandinavian Journal of Statistics*, 39:743–756, 2012.
- J. Cussens. Bayesian network learning with cutting planes. In *Twenty-seventh Conference on Uncertainty in Artificial Intelligence*, pages 153–160, 2011.
- J. Cussens, M. Järvisalo, J. H. Korhonen, and M. Bartlett. Bayesian network structure learning with integer programming: Polytopes, facets, and complexity. *Journal of Artificial Intelligence Research*, 58:185–229, 2017.
- A. P. Dawid. Beware of the DAG! *Journal of Machine Learning Research Workshop and Conference Proceedings*, 6:59–86, 2010.
- D. Eaton and K. Murphy. Bayesian structure learning using dynamic programming and MCMC. In *Twenty-third Conference on Uncertainty in Artificial Intelligence*, pages 101–108, 2007.
- F. Elwert. Graphical causal models. In *Handbook of causal analysis for social research*, pages 245–273. Springer, 2013.
- N. Friedman. Inferring cellular networks using probabilistic graphical models. *Science*, 303:799–805, 2004.
- N. Friedman and D. Koller. Being Bayesian about network structure. A Bayesian approach to structure discovery in Bayesian networks. *Machine Learning*, 50:95–125, 2003.
- N. Friedman, I. Nachman, and D. Pe’er. Learning Bayesian network structure from massive datasets: the “sparse candidate” algorithm. In *Fifteenth Conference on Uncertainty in Artificial Intelligence*, pages 206–215, 1999.
- N. Friedman, M. Linial, I. Nachman, and D. Pe’er. Using Bayesian networks to analyze expression data. *Journal of Computational Biology*, 7:601–620, 2000.

- D. Geiger and D. Heckerman. Parameter priors for directed acyclic graphical models and the characterization of several probability distributions. *Annals of Statistics*, 30:1412–1440, 2002.
- P. Giudici and R. Castelo. Improving Markov chain Monte Carlo model search for data mining. *Machine Learning*, 50:127–158, 2003.
- R. J. B. Goudie and S. Mukherjee. A Gibbs sampler for learning DAGs. *Journal of Machine Learning Research*, 17:1032–1070, 2016.
- Sander Greenland, Judea Pearl, and James M Robins. Causal diagrams for epidemiologic research. *Epidemiology*, pages 37–48, 1999.
- M. Grzegorzczuk and D. Husmeier. Improving the structure MCMC sampler for Bayesian networks by introducing a new edge reversal move. *Machine Learning*, 71:265–305, 2008.
- R. He, J. Tian, and H. Wu. Structure learning in Bayesian networks of moderate size by efficient sampling. *Journal of Machine Learning Research*, 17:3483–3536, 2016.
- D. Heckerman and D. Geiger. Learning Bayesian networks: A unification for discrete and Gaussian domains. In *Eleventh Conference on Uncertainty in Artificial Intelligence*, pages 274–284, 1995.
- D. Heckerman, C. Meek, and G. Cooper. A Bayesian approach to causal discovery. *Innovations in Machine Learning*, pages 1–28, 2006.
- M. A. Hernán and J. M. Robins. Instruments for causal inference: an epidemiologist’s dream? *Epidemiology*, 17:360–372, 2006.
- D. Jennings and J. N. Corcoran. A birth and death process for Bayesian network structure inference. *Probability in the Engineering and Informational Sciences*, 32:615–625, 2018.
- M. Kalisch and P. Bühlmann. Estimating high-dimensional directed acyclic graphs with the PC-algorithm. *Journal of Machine Learning Research*, 8:613–636, 2007.
- M. Kalisch, M. Mächler, D. Colombo, M. H. Maathuis, and P. Bühlmann. Causal inference using graphical models with the R package pcalg. *Journal of Statistical Software*, 47: 1–26, 2012.
- M. Koivisto and K. Sood. Exact Bayesian structure discovery in Bayesian networks. *Journal of Machine Learning Research*, 5:549–573, 2004.
- D. Koller and N. Friedman. *Probabilistic graphical models*. MIT press, 2009.
- J. Kuipers and G. Moffa. Uniform random generation of large acyclic digraphs. *Statistics and Computing*, 25:227–242, 2015.
- J. Kuipers and G. Moffa. Partition MCMC for inference on acyclic digraphs. *Journal of the American Statistical Association*, 112:282–299, 2017.

- J. Kuipers, G. Moffa, and D. Heckerman. Addendum on the scoring of Gaussian directed acyclic graphical models. *Annals of Statistics*, 42:1689–1691, 2014.
- J. Kuipers, T. Thurnherr, G. Moffa, P. Suter, J. Behr, R. Goosen, G. Christofori, and N. Beerenwinkel. Mutational interactions define novel cancer subgroups. *Nature Communications*, 9:4353, 2018.
- M. H. Maathuis, M. Kalisch, and P. Bühlmann. Estimating high-dimensional intervention effects from observational data. *Annals of Statistics*, 37:3133–3164, 2009.
- D. Madigan and J. York. Bayesian graphical models for discrete data. *International Statistical Review*, 63:215–232, 1995.
- C. Meek. Causal inference and causal explanation with background knowledge. In *Eleventh Conference on Uncertainty in Artificial Intelligence*, pages 403–410, 1995.
- G. Moffa, G. Catone, J. Kuipers, E. Kuipers, D. Freeman, S. Marwaha, B. Lennox, M. Broome, and P. Bebbington. Using directed acyclic graphs in epidemiological research in psychosis: An analysis of the role of bullying in psychosis. *Schizophrenia Bulletin*, 43:1273–1279, 2017.
- P. Nandy, A. Hauser, and M. H. Maathuis. High-dimensional consistency in score-based and hybrid structure learning. *Annals of Statistics*, 46:3151–3183, 2018.
- J. Pearl. *Causality: models, reasoning and inference*. MIT press, 2000.
- R Core Team. *R: A Language and Environment for Statistical Computing*. R Foundation for Statistical Computing, 2017. URL <https://www.R-project.org/>.
- G. Raskutti and C. Uhler. Learning directed acyclic graphs based on sparsest permutations. *Stat*, 7:e183, 2018.
- R. W. Robinson. Enumeration of acyclic digraphs. In *Second Chapel Hill Conference on Combinatorial Mathematics and its Applications*, pages 391–399, 1970.
- R. W. Robinson. Counting labeled acyclic digraphs. In *New directions in the theory of graphs*, pages 239–273. Academic Press, New York, 1973.
- M. Scanagatta, C. P. de Campos, G. Corani, and M. Zaffalon. Learning Bayesian networks with thousands of variables. In *Advances in Neural Information Processing Systems*, pages 1864–1872, 2015.
- M. Scutari. Learning Bayesian networks with the bnlearn R package. *Journal of Statistical Software*, 35:1–22, 2010.
- T. Silander and P. Myllymäki. A simple approach for finding the globally optimal Bayesian network structure. In *Twenty-second Conference on Uncertainty in Artificial Intelligence*, pages 445–452, 2006.
- P. Spirtes, C. N. Glymour, and R. Scheines. *Causation, prediction, and search*. MIT Press, 2000.

- M. Teyssier and D. Koller. Ordering-based search: A simple and effective algorithm for learning Bayesian networks. In *Twenty-first Conference on Uncertainty in Artificial Intelligence*, pages 584–590, 2005.
- I. Tsamardinos, L. E. Brown, and C. F. Aliferis. The max-min hill-climbing Bayesian network structure learning algorithm. *Machine Learning*, 65:31–78, 2006.
- C. Uhler, G. Raskutti, P. Bühlmann, and B. Yu. Geometry of faithfulness assumption in causal inference. *Annals of Statistics*, 41:436–463, 2013.
- T. J. VanderWeele and J. M. Robins. Four types of effect modification: A classification based on directed acyclic graphs. *Epidemiology*, 18:561–568, 2007.
- T. S. Verma and J. Pearl. Equivalence and synthesis of causal models. In *Sixth Conference on Uncertainty in Artificial Intelligence*, pages 220–227, 1990.